Towards a combinatorial algorithm for the enumeration of isotopy classes of symmetric cellular embeddings of graphs on hyperbolic surfaces

Benedikt Kolbe

Towards a combinatorial algorithm for the enumeration of isotopy classes of symmetric cellular embeddings of graphs on hyperbolic surfaces

Benedikt Kolbe
Hausdorff Center for Mathematics, University of Bonn

Abstract

Based on the recent mathematical theory of isotopic tilings, we present the, to the best of our knowledge, first algorithm for the enumeration of isotopy classes of cellular embeddings of graphs invariant under a given symmetry group on hyperbolic surfaces. To achieve this, we substitute the isotopy classes with combinatorial objects and propose different techniques, guided by structural results on the mapping class group of an orbifold and notions from computational group theory that ensure that the algorithm is computationally tractable. Furthermore, we extend data structures of combinatorial tiling theory to isotopy classes that lead to an actual implementation of the algorithm for symmetry groups generated by rotations.
From the enumerated combinatorial objects, we produce a range of simple graphs on hyperbolic surfaces represented as symmetric tilings in the hyperbolic plane, illustrating the enumeration with examples and experimentally demonstrating the feasibility of the approach. These tilings are finally projected onto a family of triply-periodic surfaces that are relevant for the natural sciences.

2012 ACM Subject Classification Mathematics of computing → Enumeration; Mathematics of computing → Geometric topology; Mathematics of computing → Graphs and surfaces; Theory of computation → Regular languages; Theory of computation → Automata over infinite objects; Mathematics of computing → Graph enumeration

Keywords and phrases Isotopic tiling theory, Delaney-Dress tiling theory, Mapping class groups, Orbifolds, Hyperbolic tilings, Enumeration, Algorithms, Automatic groups, Computational group theory, Coset enumeration, Data structure, Geodesic languages, Cayley graphs

Funding This work was partially supported by grant ANR-17-CE40-0033 of the French National Research Agency ANR (project SoS) `https://SoS.loria.fr/`.
Benedikt Kolbe: This work was done while the author was working at Université de Lorraine, CNRS, Inria, LORIA, F-54000 Nancy, France

Acknowledgements We want to thank Myfanwy Evans, John Sullivan, Vanessa Robins, Stuart Ramsden, Martin Pedersen, and Stephen Hyde for countless fruitful discussions concerning enumerations of symmetrically embedded graph over many years.

1 Introduction and motivation

The use of graphs embedded on hyperbolic surfaces to describe complicated three-dimensional structures in both structural chemistry and polymer self-assembly has recently garnered growing attention from different fields [47, 63, 51, 52, 26, 7, 53, 54, 13]. Assemblies of molecules in energetically favorable crystalline arrangements involve curvature [41], and many chemical structures have been found to reticulate triply-periodic minimal surfaces (TPMS) [39, 40], which are minimal surfaces in $\mathbb{R}^3$ invariant under three linearly independent translations, i.e. a lattice L_3 [71].

These observations have spurred the development of the EPINET [1] (Euclidean patterns in non-euclidean tilings) project, where TPMS are used as a scaffold for symmetrically

embedded graphs, for the enumeration and subsequent analysis of crystallographic nets (triply-periodic connected graphs) and polyhedra in $\mathbb{R}^3$ [68, 62, 67, 42, 66, 11, 3].

TPMS are associated to the closed surface S_g of genus g in the 3-torus $\mathbb{T}^3 = \mathbb{R}^3/L_3$ obtained by gluing the TPMS along the equivalent faces of a translational domain for L_3. It turns out that S_g is always intrinsically hyperbolic [59]. The gyroid, the primitive, and the diamond TPMS are arguably the most prominent examples of TPMS [72, 45, 48, 19, 31, 75]. The symmetries of every closed Riemannian surface S_g with genus $g > 1$ can be described as hyperbolic symmetries, by the celebrated uniformization theorem [5], [55, Lemma 2.2.1], such that the fundamental group $\pi_1(S_g)$ can be identified with a discrete group of hyperbolic translations and embedded graphs on S_g can be depicted as tilings of $\mathbb{H}^2$.

Figure 1(a)-(c) illustrates the covering, by the hyperbolic plane $\mathbb{H}^2$, of the closed surface S_D giving rise to the diamond TPMS. The fundamental group $\pi_1(S_D)$ of S_D is generated by the hyperbolic translations that map opposite edges to each other. The in-surface symmetries of TPMS manifest as ambient Euclidean symmetries of $\mathbb{R}^3$ [65, Theorem 2.2.5], so that symmetric graphs on TPMS give rise to symmetric nets in $\mathbb{R}^3$. Figure 1(a) shows the symmetries $\pi_1(S_D)$ of the covering map of $\mathbb{H}^2$ onto the diamond TPMS, i.e. elements in $\pi_1(S_D)$. The triangles in (b) and (c) illustrate the symmetries of the diamond TPMS, in $\mathbb{H}^2$ and in $\mathbb{R}^3$, respectively. In $\mathbb{H}^2$, the symmetries of the diamond TPMS correspond to elements of the symmetry group $*246$, following Conway's orbifold notation [15] (Appendix A).

The EPINET approach can be summarized as in Figure 1(d)-(f), where (d) shows a colored hyperbolic tiling that is the lift of a graph embedded in the *orbifold* associated to the symmetry group of the tiling. The red and green edges forming the boundary of the tile project to a graph on the TPMS, which, upon discarding the surface, yields the net in (f).

An essential tool of the enumerative process is what is referred to as *combinatorial tiling theory* [21, 20], a field that has been investigated from an algorithmic point of view [37, 16, 76], with data structures and algorithms that allow for analyses, manipulations and enumerations of combinatorial objects, called *D-symbols*, complete invariants for equivariant equivalence classes of tilings (Section 2) of simply connected spaces by compact disks. On surfaces, the strictly weaker notion of isotopy becomes the natural equivalence of embedded graphs to consider, where graphs that can be transformed into each other through continuous deformations are considered equivalent.

Several simple cases of hyperbolic tilings and their isotopy classes (Section 2) have been explored [46, 66, 43, 38, 45, 49, 44, 64, 63, 24, 25, 23], and resulting structures have been used in analyses in real physical systems [52]. The recent advent of new techniques arising from the theory of isotopic tilings on hyperbolic surfaces [53] and the subsequent development of a more practical framework [54] provide the mathematical foundations of a systemic approach to the enumeration of isotopy classes of tilings with a given symmetry group.

What is missing in these developments is more than a simple implementation. The purpose of this paper is to fill the missing gaps to present the, to the best of our knowledge, first algorithm for the enumeration of isotopy classes of tilings with a given symmetry group on a hyperbolic surface. While the theory encompasses arbitrary symmetry groups, our main focus will be on *stellate groups*, i.e. symmetry groups that can be generated solely by rotations, a first important step for applications. By relying on the established mathematical framework, the main issues to overcome are

1. assimilating known results to propose a combinatorial algorithm for the enumeration,
2. proposing a data structure for tilings that allows for the concrete construction of a representative of a given isotopy class of tilings,
3. investigating the feasibility of the proposed algorithms,

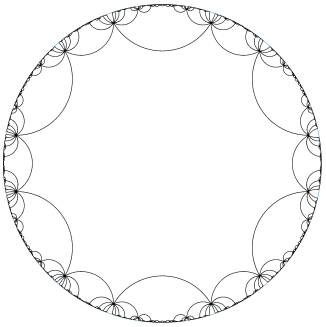

(a) Tiling of $\mathbb{H}^2$ by dodecagons corresponding to the genus 3 surface that gives rise to the diamond TPMS [54, Figure 1].

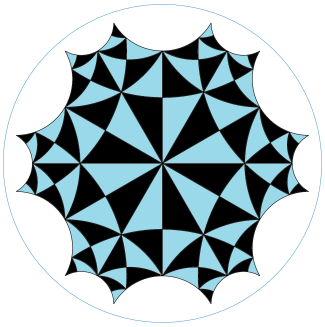

(b) The symmetries of the diamond TPMS within a unit cell, in $\mathbb{H}^2$ [54, Figure 1]. Each arc represents a mirror symmetry.

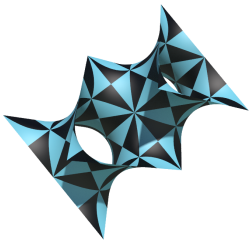

(c) A section of the diamond TPMS in $\mathbb{R}^3$, together with its smallest asymmetric triangle patches [54, Figure 1].

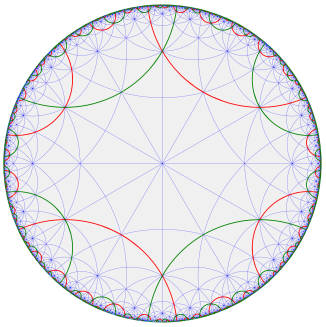

(d) A tiling of the hyperbolic plane with symmetry group 22222, represented by the green and red edges, with $*246$ triangles in blue in the background.

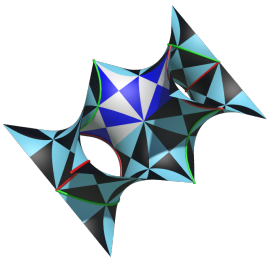

(e) The decoration from (d) and a fundamental domain of 22222 shown as a collection of dark blue and grey triangles on the diamond TPMS.

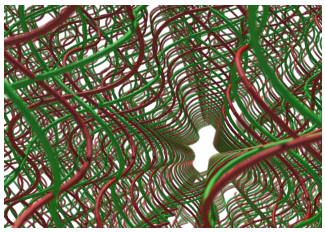

(f) The resulting net in $\mathbb{R}^3$ when the tile boundaries are taken as trajectories in Euclidean 3-space, after enforcing the translational symmetries.

Figure 1 (a)-(c) shows symmetries of the diamond TPMS in $\mathbb{R}^3$ and its uniformization in $\mathbb{H}^2$. (d)-(f) shows the progression from a tiling of the hyperbolic plane to a 3-dimensional net via a decoration of the Diamond triply-periodic minimal surface.

4. implementing the algorithm to produce tilings of $\mathbb{H}^2$ representing symmetric graph embeddings on a given hyperbolic surface S,
5. projecting the tilings in $\mathbb{H}^2$ onto the surface S.

The main contributions of this paper are solutions to the above challenges for stellate groups and the prominent class of TPMS containing the gyroid and others, which serves as a concrete example illustrating our techniques. More concretely, after having laid the theoretical groundwork (Sections 2, 3.1 and 3.2) we present Algorithms 1 and 2 for the enumeration of different classes of tilings as combinatorial objects, Algorithm 3 to produce the encoded tilings, prove a central result (Theorem 8) on the representability of tilings that is the basis of the proposed data structure, and briefly describe some of the guiding principles behind the implementation of the proposed algorithms (Sections 5). Furthermore, we present an array of examples illustrating the use of algorithm and project the produced tilings onto the diamond TPMS (Section 6).

2 Isotopic tiling theory

Isotopic tiling theory [53] describes the structure of symmetric cellular embeddings of graphs up to deformations on a hyperbolic surface S, i.e. embeddings, for which the complement is homeomorphic to a set of open disks, which are moreover invariant under a group of symmetries. We briefly recall the relevant definitions and basic results.

The first idea at the heart of the theory is to replace embedded graphs on S with the study of tilings in the universal covering space $\mathbb{H}^2$. A countable set $\mathcal{T}$ of compact disks in $\mathbb{H}^2$ is called a *tiling* if every point $x \in \mathbb{H}^2$ belongs to at least one tile $T \in \mathcal{T}$, every two tiles T_1 and T_2 of $\mathcal{T}$ have disjoint interior, and the collection of tiles is locally finite[1]. A *vertex* is a point that is contained in at least three tiles, and an *edge* is a connected segment of tile boundary joining two vertices.

Let $\mathcal{T}$ be a tiling of $\mathbb{H}^2$ and let Γ be a *symmetry group*, i.e. a discrete group of isometries of $\mathbb{H}^2$ with compact quotient space. If $\mathcal{T} = \gamma\mathcal{T} := \{\gamma T \mid T \in \mathcal{T}\}$ for all $\gamma \in \Gamma$ then we call Γ a symmetry group of $\mathcal{T}$ and the pair $(\mathcal{T}, \Gamma)$ an *equivariant tiling*. The *orbit* of a tile(edge,vertex) T is the subset of $\mathcal{T}$ given by images of T: $\Gamma.T = \{\gamma T \text{ for } \gamma \in \Gamma\}$. For a given tile (vertex, edge) $T \in \mathcal{T}$, the *stabilizer subgroup* Γ_T is the subgroup of Γ that fixes T, i.e. $\Gamma_T = \{\gamma \in \Gamma \mid \gamma T = T\}$. A tile is called *fundamental* if Γ_T is trivial and the whole tiling is fundamental if this is true for all tiles. An equivariant tiling is called *tile-k-transitive*, when k is the number of distinct orbits of tiles under the action of Γ. To simplify language, we also call fundamental tile-1-transitive tilings *1-fundamental tilings*. Any tile in a 1-fundamental tiling $(\mathcal{T}, \Gamma)$ is the closure of a fundamental domain for Γ and conversely, any closed fundamental domain for Γ gives rise to such a tiling. A *colored tiling* is a tiling where each edge orbit is colored differently, for distinguishability. It turns out that restricting to colored tilings simplifies some of the steps of our algorithms.

Lifting a cellular embedding of a graph on S clearly gives rise to an equivariant tiling. The following converse statement is implicit in [53]. We refer to Appendix B for a proof.

▶ **Proposition 1.** *The edge graph of the tiling $(\mathcal{T}, \pi_1(S))$, with $\pi_1(S)$ the fundamental group of a hyperbolic surface S, projects to a cellular embedding of some graph on S.*

In view of Proposition 1, we refer to projections of tilings to S as tilings of S.

[1] A collection of sets is locally finite if any compact set meets only a finite number of sets in the collection.

For now on, let $\mathcal{O}_\Gamma$ be a compact *(hyperbolic) orbifold* with symmetry group $\Gamma \subset \mathrm{Iso}(\mathbb{H}^2)$, and $O_\Gamma = \mathbb{H}^2/\Gamma$ its underlying topological space. The orbifold $\mathcal{O}_\Gamma$ can be thought of as the quotient space O_Γ together a label for each point corresponding to the isomorphism class of its stabilizer subgroup in Γ. Appendix A provides further details.

▶ **Definition 2** ([53]). *Two equivariant tilings* $(\mathcal{T}_1, \Gamma_1)$ *and* $(\mathcal{T}_2, \Gamma_2)$ *of* $\mathbb{H}^2$ *are* equivariantly equivalent *if there is a homeomorphism* ϕ *of* $\mathbb{H}^2$ *s.t.* $\phi(T_1) \in \mathcal{T}_2$ *and* ϕ *is* equivariant*, i.e. if there is a group isomorphism* $h : \Gamma_1 \to \Gamma_2$ *s.t.* $h(\gamma_1)(\phi(T_1)) = \phi(\gamma_1 T_1)$ *for all* $\gamma_1 \in \Gamma_1$ *and* $T_1 \in \mathcal{T}_1$*. If* $\Gamma_1 = \Gamma_2$ *and there exists a* Γ_1*-equivariant homeomorphism* ϕ *as above that is isotopic to the identity through a (continuous) path of (*Γ_1*-)equivariant homeomorphisms, the two tilings are called* isotopically equivalent*.*

Tilings of a hyperbolic surface S are isotopically equivalent w.r.t. any group of isometries of S exactly when the tilings can be deformed into one another on S [53, Prop. 3].

Dress [21] showed that a complete invariant for equivariant equivalence, called the D-symbol, exists for tilings of simply connected manifolds, which can be constructed explicitly from a given tiling using the tiles and the symmetry group. The D-symbol consists of a finite graph that records adjacencies between tiles and their faces, augmented by weights that encode the group action of Γ on $\mathcal{T}$. We will not need the exact definition for our purposes, only that a D-symbol has as many vertices as orbits of flags (triples consisting of a mutually incident vertex, edge and tile) in the tiling, and that two equivariant tilings are equivariantly equivalent if and only if their D-symbols are isomorphic as weighted graphs [37, Lemma 1.1].

D-symbols can be exploited for a fully algorithmic approach to the enumeration and identification up to equivariant equivalence of tilings in $\mathbb{H}^2$, starting from 1-fundamental tilings, by assigning a *size*, a measure of complexity for D-symbols and substituting each tiling with its respective D-symbol [37, 16]. The enumeration is then based on the result [37] that fundamental tile-k-transitive tilings are derived from fundamental tile-$(k-1)$-transitive tilings using the operation *SPLIT*, which inserts an edge into a fundamental tile. Non-fundamental tile-k-transitive tilings are obtained from fundamental ones by *GLUE*, where one glues equivalent tiles in a tiling by removing edges that separate them. The GLUE and SPLIT operations extend to enumerations of isotopy classes of equivariant tilings [53, Prop. 1].

The MCG $\mathrm{Mod}(\mathcal{O}_\Gamma)$ of an orbifold $\mathcal{O}_\Gamma$ can be defined as the group of Γ-equivariant homeomorphisms of $\mathbb{H}^2$, modulo isotopies preserving Γ, i.e. two such homeomorphisms are identified if they can be joined by a path of Γ-equivariant homeomorphisms [53]. We also say that they are isotopic in $\mathcal{O}_\Gamma$, since a Γ-equivariant homeomorphism corresponds to a homeomorphism of $\mathcal{O}_\Gamma$. A fact we will make use of is that MCGs only depend on the number of the different types of symbols in its Conway name, so, for example, 2223 and 4447 have isomorphic MCGs, as do 2366 and 5799, but not 2244 and 2222. We shall refer to the extensively studied [27] MCGs of closed orientable surfaces, possibly with punctures, as *classical MCGs*. The subgroup of homeomorphisms that preserve the orientation of $\mathbb{H}^2$ is known as the *orientable MCG* $\mathrm{Mod}^+(\mathcal{O}_\Gamma)$.

2.1 The MCG and enumerations of isotopy classes

The main takeaway from isotopic tiling theory for our purposes is that $\mathrm{Mod}(\mathcal{O}_\Gamma)$ acts transitively on the set of isotopy classes associated to $(\mathcal{T}, \Gamma)$ [53, Prop. 1]. The elements of $\mathrm{Mod}(\mathcal{O}_\Gamma)$ in turn coincide with certain sets of generators for Γ, defined up to conjugacy [53, Theorem 2]. The relevant sets of generators can be computed explicitly from a single starting set using the action of the MCG on sets of generators, which was recently derived using special sets of generators for the MCG [54]. We can summarize this as follows.

▶ **Theorem 3.** *An isotopy class of tilings can be encoded combinatorially by its D-symbol, a given starting set of generators, and an element of the MCG of its symmetry group.*

For a stellate symmetry group with given Conway symbol, the sets of generators we consider for the enumeration is the set consisting of one rotation for every symbol in its name and we will subsequently always mean such a set when we talk about generators of a stellate group. For example, for the group 2224 the set of relevant generators consists of three 2-fold rotations and a single 4-fold rotation. These rotations are uniquely determined by their orders and where their fixed points lie in $\mathbb{H}^2$. Figure 10 shows an example of how different sets of such generators of a given group with symbol 2224 gives rise to different representatives of isotopy classes of tilings. The positions of the fixed points of the 2-fold rotations are marked by the numbers 1 to 3 and the fourfold rotation is marked with a 4. In each case, the tiling is a result of joining, with a geodesic, the fixed point marked by 1 to those marked by 2 and 4, and likewise from 4 to 3. Each of the depicted tilings project to tilings of the surface S_D from the introduction, with the dodecagon shown on the left.

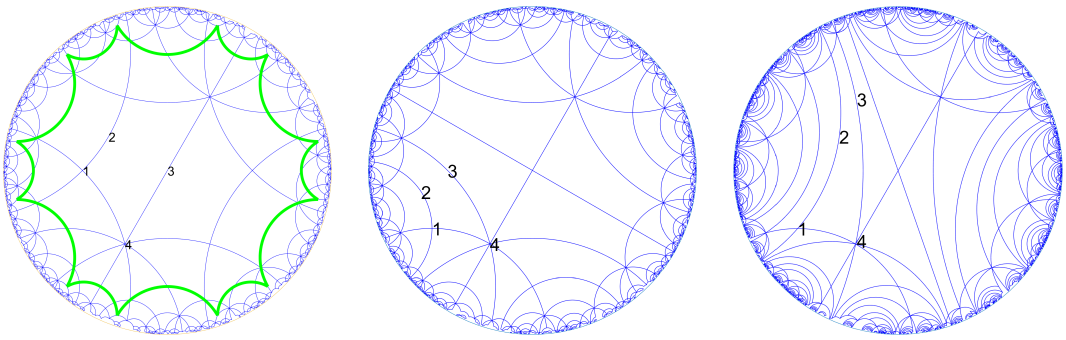

Figure 2 Isotopically distinct fundamental tilings with symmetry group 2224 and same D-symbol, from a fixed way of connecting generators with geodesics. They all project to tilings of the surface obtained by gluing opposite edges of the dodecagon shown on the left.

3 The algorithm for enumerations of isotopy classes of tilings

Before presenting the enumeration algorithm, we discuss some preliminaries.

3.1 Stabilizer subgroups of the action of the MCG on isotopy classes

The stabilizer subgroup of the action of the MCG on an isotopy class of tilings $(\mathcal{T}, \Gamma)$ is finite [53, Proposition 5]. Furthermore, a nontrivial stabilizer subgroup corresponds to a finite group of additional symmetries of a tiling $(\mathcal{T}', \Gamma')$ equivariantly equivalent to $(\mathcal{T}, \Gamma)$, i.e. Γ' is not the maximal group of symmetries of $\mathcal{T}'$ [53, Theorem 4]. This situation can be identified by the existence of a nontrivial graph automorphism of the D-symbol associated to tiling [20], with available algorithms and implementations [16, Section 3].

▶ **Proposition 4.** *Let $\mathcal{T}_c$ be a colored tiling associated to $(\mathcal{T}, \Gamma)$. Then the stabilizer subgroup of $\mathcal{T}_c$ in the orientable MCG is trivial.*

It is possible for a nontrivial orientation reversing homeomorphism to act trivially on a colored tiling, as illustrated by the reflection across the center line in Figure 5 below.

Proof. We first show that it is sufficient to show the statement for orientable orbifolds. The orbifold $\mathcal{O}_{\Gamma^+}$, where Γ^+ is the index two subgroup of Γ consisting of the orientation preserving isometries in Γ, is known as the oriented double cover of $\mathcal{O}_\Gamma$. A result that can be considered folklore (see Appendix C) states that for every homemophism f of $\mathcal{O}_\Gamma$, there is an orientation preserving homeomorphism $\tilde{f}$ of $\mathcal{O}_{\Gamma^+}$ that lifts f. Thus, if the statement of the proposition holds for $\mathcal{O}_{\Gamma^+}$, then we conclude that $\tilde{f}$ is isotopically trivial in $\mathcal{O}_{\Gamma^+}$, and thus f is trivial in $\mathrm{Mod}^+(\mathcal{O}_\Gamma)$ [53, Proposition 3].

For orientable orbifolds, the statement follows from the well-known Alexander method [74, Prop. 8.5], by Proposition 1. To apply the method, we may consider some of the vertices of the graph of tile edges in $\mathcal{T}$ projected to $\mathcal{O}_\Gamma$ as marked points. ◀

▶ **Corollary 5.** *The full stabilizer subgroup of a colored tiling $\mathcal{T}_c$ is either trivial or of order 2.*

Proof. If r_1, r_2 are two orientation reversing homeomorphisms with $r_1(\mathcal{T}_c) = \mathcal{T}_c = r_2(\mathcal{T}_c)$, then $r_1^{-1} r_2(\mathcal{T}_c) = \mathcal{T}_c$, so they represent the same element in the MCG, by Proposition 4. ◀

On the side of MCGs, results on the structure of finite subgroups of MCGs can be used to identify candidates of subgroups of the MCG that account exactly for the ambiguities in the list of isotopy classes of a given tiling on a hyperbolic surface [53, Section 7]. For stellate groups, the possible finite order elements have been completely classified and are explicitly known in terms of certain generators of the MCG [56, Theorem 4.4]. For general symmetry groups, however, the problem of classifying all finite subgroups of the MCG in similar ways is an active area of research, with recent progress for genus 2 closed surfaces [61].

▶ **Lemma 6.** *Given an equivariant tiling $(\mathcal{T}, \Gamma)$, the set $E = \mathrm{Mod}(\mathcal{O}_\Gamma)/M_\mathcal{T}$, where $M_\mathcal{T} \subset \mathrm{Mod}(\mathcal{O}_\Gamma)$ is the stabilizer subgroup in $\mathrm{Mod}(\mathcal{O}_\Gamma)$ of $\mathcal{T}$, is an unambiguous enumeration of isotopy classes of tilings associated to $(\mathcal{T}, \Gamma)$.*

Proof. The MCG acts transitively on isotopy classes, so we only show that the enumeration is unambiguous. For $[m_1], [m_2] \in E$ s.t. $[m_1]\mathcal{T} = [m_2]\mathcal{T}$, $[m_1]^{-1}[m_2] \in M_\mathcal{T}$, so $[m_1] = [m_2]$. ◀

By Lemma 6, for an enumeration of isotopy classes of tilings in $\mathbb{H}^2$ with symmetry group Γ using the MCG, one generally needs to enumerate cosets of the MCG w.r.t. finite subgroups.

3.2 Finding the possible symmetry groups of a graph embedding

To make use of isotopic tiling theory for the enumeration of isotopy classes of symmetric cellular graph embeddings on a hyperbolic surface, we first need to identify the possible symmetry groups of the tilings they represent, as they will be part of the input of Algorithms 1 and 2 below. Any hyperbolic surface admits a finite group of isometries that contains all isometries of the surface, by Hurwitz's theorem [27, Theorem 7.4, Proposition 7.7]. Therefore, for a given hyperbolic surface $S = \mathbb{H}^2/\pi_1(\mathrm{S})$ with fundamental group $\pi_1(\mathrm{S})$, there is a maximal symmetry group Γ_M with $\pi_1(\mathrm{S}) \subset \Gamma_M$ such that any tiling on S lifts to a tiling in $\mathbb{H}^2$ with a *commensurate* symmetry group Γ, i.e., such that

$$\pi_1(\mathrm{S}) \subset \Gamma \subset \Gamma_M. \tag{1}$$

Conversely, if a tiling $\mathcal{T}$ has Γ satisfying (1) as its symmetry group, then it is *commensurate* with S, i.e., invariant under $\pi_1(\mathrm{S})$, and will project to a tiling $\mathcal{T}_S$ on S.

Finding all groups Γ that satisfy (1) is simpler if S is the hyperbolic surface associated to a TPMS, since it turns out that in this case $\pi_1(\mathrm{S})$ is normal in Γ_M [54, Section 2.3]. To see this, note that the symmetries of S are realized by ambient isometries in $\mathbb{R}^3$ in the embedding

as a TPMS, as mentioned in the introduction. Therefore, there is an isomorphism Ψ from Γ_M to a group of Euclidean motions, with $\Psi(\pi_1(\mathrm{S}))$ being equal to the lattice L_3 containing all translations under which the TPMS is invariant. Conjugation of a translation in $\mathbb{R}^3$ by a symmetry of the TPMS yields a translation, necessarily contained in L_3, so we see that L_3 is normal in $\Psi(\Gamma_M)$, and thus so is $\pi_1(\mathrm{S})$ in Γ_M.

By normality, each subgroup Γ satisfying (1) corresponds uniquely to a subgroup of the finite group $\Gamma_M/\pi_1(\mathrm{S})$ [34, Lemma 2.7.5]. Therefore, to list all possible symmetry groups for a tiling on S, we list all of the finitely many possible subgroups of $\Gamma_M/\pi_1(\mathrm{S})$. This is accomplished using existing algorithms and their implementations available in the GAP programming language [30], from a finite presentation of $\Gamma_M/\pi_1(\mathrm{S})$. To obtain a finite presentation of $\Gamma_M/\pi_1(\mathrm{S})$, we use the group presentation associated to the orbifold symbol of Γ_M and express the generators of $\pi_1(\mathrm{S})$ in terms of these. The output is a presentation of the subgroups in the generators of the input presentation, to which we add the generators of $\pi_1(\mathrm{S})$ as words in the generators of Γ_M to obtain a presentation of each symmetry group on S as a group of isometries of $\mathbb{H}^2$ containing $\pi_1(\mathrm{S})$. For the diamond surface family and its associated surface S_D from Figure 1, there are 131 subgroups Γ satisfying $\pi_1(\mathrm{S}) \subset \Gamma \subset \Gamma_M = *246$, up to conjugacy in $*246$, the maximal symmetry group of S_D. These have been completely listed using a special case of the methods described here in the case of S_D [67]; we refer to these commensurate subgroups by their numbers in the resulting list. The stellate groups contained in this list are as follows: 246, 266, 344, 2223, 2224, 2226, 2233, 2244, 2266, 4444, 22222, 22223, 2222222, and 22222222. Note that these 14 groups feature 8 nontrivial different MCGs (the MCG of 246 is trivial [54]). Note that these groups can occur more than once as commensurate subgroups of Γ_M, even as nonconjugate versions. For example, the group 22222 occurs three times, as groups 54, 76, and 77 in the list of nonconjugate commensurate subgroups of $*246$. The interest in restricting attention to one symmetry group in every conjugacy class comes from the fact that all symmetries in $*246$ lift to isometries of $\mathbb{R}^3$ in an embedding as a TPMS, as mentioned above.

The enumeration algorithms

We now formulate the main result of this paper: An algorithm for the enumeration of isotopy classes of tilings by disks with a given symmetry group up to a particular complexity. We will present two different flavors of the algorithm, of independent interest. Apart from the symmetry group Γ of the tilings, found using the methods described in Section 3.2, the input of the algorithm is the highest complexity of the D-symbol up to which we enumerate, a presentation of the MCG $\mathrm{Mod}(\mathcal{O}_\Gamma)$ and a word length up to which we enumerate the different isotopy classes of tilings as elements (representing cosets) of the MCG. We break up the two algorithms into two parts. The first produces the isotopy classes as combinatorial objects as in Theorem 3 and the second produces an actual tiling for each element in the list.

A closely related and somewhat simpler algorithm enumerates combinatorial objects representing isotopy classes of colored tilings:

Step 1 in both algorithms has been treated in the literature and can be carried out using known algorithms as explained in Section 2. A recent implementation is publicly available and has led to a database of equivariant equivalence classes of tilings [76]. Lemma 6 shows that the enumeration of isotopy classes using cosets is complete and unambiguous, and Proposition 4 and Corollary 5 show that colored tilings are at most invariant under an orientation reversing homeomorphism of order two. Together with Theorem 3 with an arbitrary starting set of generators, we obtain Theorem 7.

Algorithm 1 Enumerating isotopy classes of a given symmetry group up to given threshold

1. List all D-symbols up to the given complexity.
2. Check for the existence of graph automorphisms of each D-symbol, as these lead to ambiguities in the action of the MCG.
3. Find the finite subgroup H in the MCG corresponding to the graph automorphism group for each D-symbol, using theoretical results on their structures.
4. Enumerate the cosets in $\mathrm{Mod}(\mathcal{O}_\Gamma)/H$ up to a given word length by listing a shortest representative of each.

Algorithm 2 Enumerating colored isotopy classes of a given symmetry group up to given threshold

1. List all D-symbols up to the given complexity.
2. Check if each D-symbol admits a graph automorphism that preserves edge colors.
3. Enumerate the elements in either $\mathrm{Mod}^+(\mathcal{O}_\Gamma)$ or the full MCG $\mathrm{Mod}(\mathcal{O}_\Gamma)$, depending on Step 2, up to a given word length by listing a shortest representative of each.

▶ **Theorem 7.** *Algorithms 1 and 2 each output a list of D-symbols and a list of elements of* $\mathrm{Mod}(\mathcal{O}_\Gamma)$ *up to the given thresholds, associated with an enumeration of isotopy classes of tilings and colored tilings, respectively.*

The second step of either algorithm can be solved using algorithms 9 and 10 in [16], which have expected quadratic time complexity in the number of vertices of the D-symbol. These algorithms work by traversing the graph representing the D-symbol and checking for possible equivalences among the vertices. Since the vertices of a D-symbol represent flags of the tilings, the algorithms can be adjusted simply by adding an extra key to each vertex storing an identifier for the color of the edge incident to the flag, prohibiting equivalences among flags with different colors.

As pointed out in Section 3.1, finding the finite subgroups corresponding to automorphisms of D-symbols in MCGs in Step 3 of Algorithm 1 leads to open problems, depending on the symmetry group of interest. For stellate groups, this step can be carried out explicitly using the characterization of all finite order elements and their orders in the associated MCG. Moreover, there is a known finite presentation of the MCG [54, Theorem 4.2] in which every generator can be expressed in the elements used in the classification of the finite order elements. In view of applications to EPINET, we focus on treating the D-symbols listed in [1] and limit our analysis of the above two algorithms to investigations of the enumeration of elements of the MCG (Section 5).

To obtain realizations as tilings in $\mathbb{H}^2$ with symmetry group Γ for each element in the output of the two algorithms, we propose Algorithm 3. The data structure we propose in the next section goes hand in hand with a practical solution to Algorithm 3.

To apply elements of the MCG to generators as in Step 3 of Algorithm 3, one can substitute elements of the MCG by algebraic transformations of generators of Γ [53, Theorem 2, Section 3], which can be explicitly derived for special sets of generators [54]. The action of the MCG can then be expressed in the form of a matrix multiplication in $\mathrm{PGL}(2,\mathbb{R})$, the group of orientation-preserving isometries of $\mathbb{H}^2$, involving only the starting set of generators. The graph embeddings in Step 4 of Algorithm 3 and therefore tilings in $\mathbb{H}^2$ can be built from combinatorial information involving a set of generators for Γ, see Section 4 below.

Algorithm 3 Produce tilings representing the output of Algorithms 1 and 2

1. Find a starting set of generators $\mathcal{G}$ for Γ.
2. For a D-symbol S, find the embedded graph in the orbifold associated to Γ and describe this embedding w.r.t. the generators.
3. Apply the elements of $\mathrm{Mod}(\mathcal{O}_\Gamma)$ in the output of Algorithms 1 and 2 to $\mathcal{G}$ using an action of the MCG on generators to obtain a list of sets of generators of Γ.
4. Embed the graphs found in Step 2 into $\mathbb{H}^2$ w.r.t. each set of generators from Step 3 and produce the corresponding tiling in $\mathbb{H}^2$ by imposing the symmetries.

4 Data structure for isotopy classes of tilings

A *geodesic representative* of an equivariant tiling $(\mathcal{T}, \Gamma)$ is an isotopically equivalent tiling with geodesic edges between the vertices. Some isotopy classes of tilings do not admit geodesic representative. See Figure 3 for examples, where the nongeodesic edges are piece-wise geodesics with one kink.

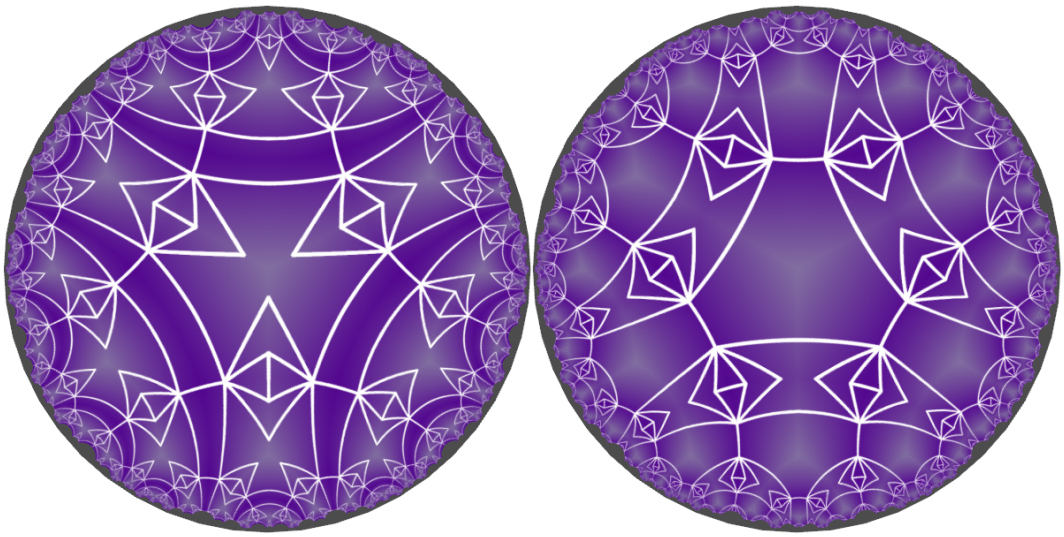

Figure 3 Two examples of tilings that cannot be transformed into tilings entirely made up of geodesics with breaks occuring only at vertices. Tilings from the EPINET database [1].

▶ **Theorem 8.** *Any isotopy class of a 1-fundamental tiling $(\mathcal{T}, \Gamma)$ has a geodesic representative. Also, if a tiling consists only of convex tiles, then it is a geodesic representative.*

The proof is somewhat technical and uses a known result that states that any simplicial complex embedded on a closed hyperbolic surface is isotopic to an embedding with only geodesic edges [14]. We defer it to Appendix F.

Theorem 8 suggests a natural data structure for 1-fundamental tilings, similar to the data structure used in SYSTRE [17] and in Delaunay triangulations in CGAL [50]. The construction of any such tiling can be carried out from the locations of vertices of any one tile in the tiling along with an adjacency matrix specifying which (copies of) these vertices to join by geodesics. An isotopy class of 1-fundamental tilings is stored as a triple $(\mathcal{G}, V, E, A)$, with $\mathcal{G}$ a finite set of generators for Γ, $V \subset \mathbb{H}^2$ representing a list of points (vertices and

possibly centers of twofold rotations) on the boundary of a tile, $E \subset V$ consisting of pairs of points, and $A \subset V$ specifying which points in V are related by an element of Γ.

We explain the proposed data structure more concretely for a stellate group Γ. The orbifold $\mathcal{O}_\Gamma$ is topologically a sphere with marked points $\{m_i\}$ that are labelled by the orders of the rotations they represent, representing the symbols present in the Conway name for Γ. The edges of any 1-fundamental tiling $\mathcal{F}$ for Γ are the result of lifting, to $\mathbb{H}^2$, a tree t in $\mathcal{O}_\Gamma$ that spans the marked points $\{m_i\}$ along with possibly other *exceptional vertices* $\{v_j\}$ of degree at least 3 and each tree yields such a tiling [57, Theorems 4.1, 5.1]. Given lifts to $\mathbb{H}^2$ of edges in t as a list of points in $\mathbb{H}^2$ to be connected to form the boundary of a tile is sufficient to reproduce the tiling by imposing the symmetries in Γ.

The proposed data structure is convenient for stellate groups: The centers of all rotations in Γ are clearly fixed by Γ-equivariant isotopies. Therefore, given a set $\mathcal{G}$ of generators of Γ, the geodesic representatives whose existence is guaranteed by Theorem 8 involves the corresponding centers, in contrast to more general symmetry groups, where the location in $\mathbb{H}^2$ of the vertices is not clear a priori and also not unique. For a tree t without exceptional vertices, i.e. that only spans points in $\{m_i\}$, the geodesic representative of the fundamental domain arising from $\mathcal{G}$ is unique in each isotopy class. Since the angles of the resulting tile are at most π, it is moreover convex. See Figure 5 for an illustration of how the corners of a fundamental domain can be expressed in terms of generators.

Figure 4 shows the nine different equivariant equivalence classes of 1-fundamental tilings of 2224 represented as tilings in $\mathbb{H}^2$, commensurate with the diamond TPMS family. The set of generators used to produce the tilings is as indicated by the indices, with the number 4 corresponding to the fourfold rotation. The first, second, third, and sixth tiling, from the top left to the bottom right, are tilings without exceptional vertices. The ordering is that of the enumeration of D-symbols [1]. The location of exceptional vertices $\tilde{v}_k$ of more complicated fundamental domains are a result of insertions of vertices into the edges of others and slight perturbations, using the convexity of fundamental domains without exceptional vertices. This step requires some experimentation as the perturbation depends on the given set of generators and the fundamental domain. However, this step does not appear to present obstructions in practice. As an example, consider the 5th tiling in Figure 4. The tree in $\mathcal{O}_\Gamma$ for the 1-fundamental tiling consists of four edges, with a degree 3 vertex v joined to marked points corresponding to 1, 2, and 4. The choice of $\tilde{v}$ (marked in the figure) was made to lie close to the geodesic between 1 and 4; the same choice works for the 4th and 8th tiling.

The proposed data structure can be extended to more general classes of tilings. Since all isotopy classes of tilings can be constructed from 1-fundamental tilings by GLUE and SPLIT operations, the SPLIT operation is the only one that presents difficulties, as the inserted edge would generally be stored as a piece-wise geodesic curve given by a sequence of points, meaning that the data structure would in general also need to store locations of points that are not vertices. Nevertheless, every isotopy class of tilings $\mathcal{T}$ can be described relative to some 1-fundamental tiling $\mathcal{F}$ together with combinatorial information on how the GLUE and SPLIT operation are successively realized on $\mathcal{F}$ to obtain $\mathcal{T}$.

4.1 Finding a starting set of generators (Step 1 of Algorithm 3)

Given a stellate group $\Gamma = \mathsf{R_1R_2...R_k}$, a natural question is which set of generators to use as a starting point for the enumeration. We answer this question in two ways.

For the first, note that there is a *Coxeter group* $\mathcal{C}$, i.e. a symmetry group generated entirely by reflections, that contains Γ as an index two subgroup, namely a group with orbifold symbol $*\mathsf{R_1R_2...R_k}$. The orbifold $\mathcal{O}_\mathcal{C}$ is topologically a disk with marked points

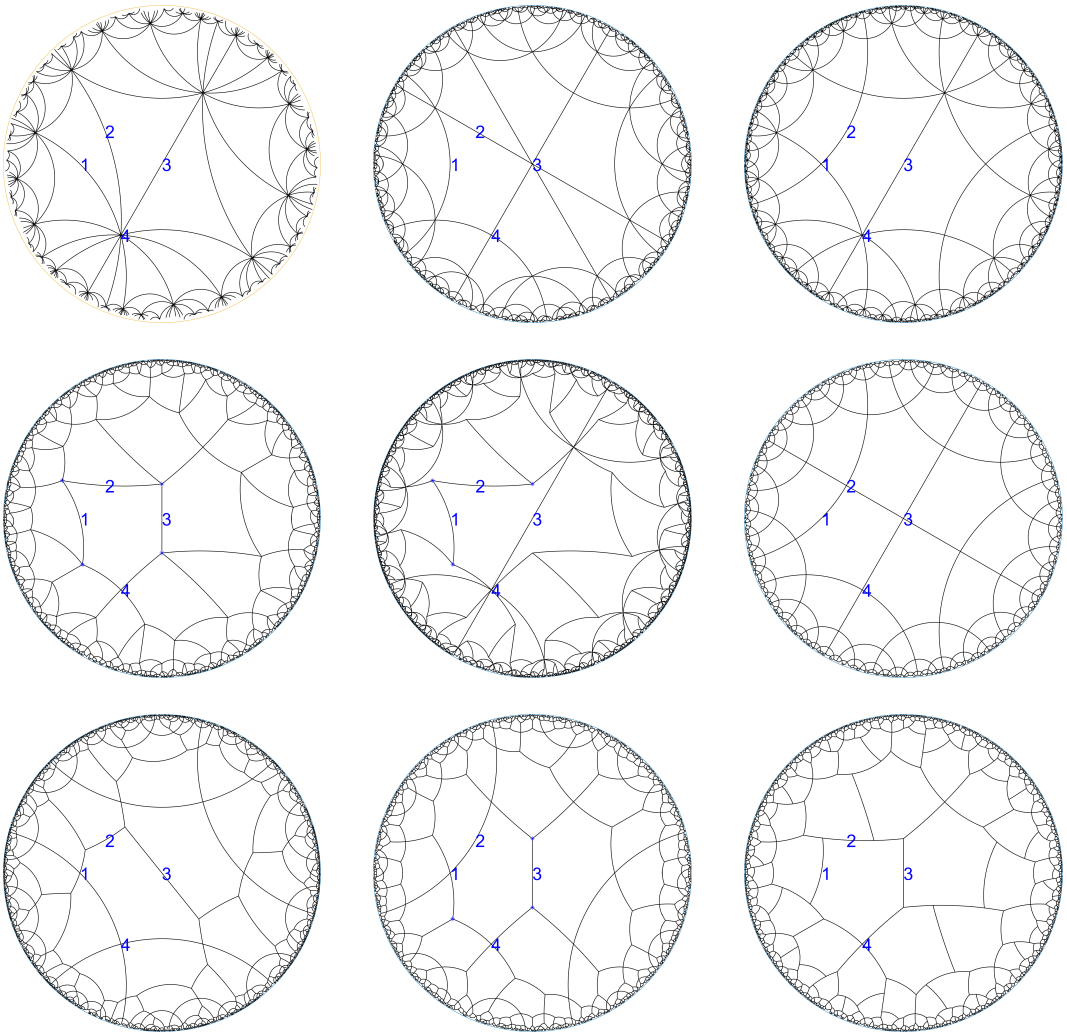

Figure 4 1-fundamental tilings with symmetry group 2224 with the 4-fold rotation located at vertex 4. The tilings represent the equivariant equivalence classes QS20(top left) to QS28(bottom right), with the naming corresponding to that in the epinet database [1].

on the boundary. The MCG is a finite group generated by homeomorphisms of the disk that map the boundary component to itself [53, p. 15]. Furthermore, there is only type of fundamental domain $F_{\mathcal{C}}$ for $*\mathsf{R}_1\mathsf{R}_2...\mathsf{R}_k$, which corresponds to an embedded graph tracing out the boundary component of $\mathcal{O}_{\mathcal{C}}$ [57, Theorem 5.1]. Therefore, there is a unique isotopy class of 1-fundamental tiling with symmetry group $\mathcal{C}$. The generators are given by hyperbolic reflections $\{M_i\}_i$ across the full geodesics in $\mathbb{H}^2$ containing geodesic arcs of the boundary of a fundamental domain $F_{\mathcal{C}}$, shown in Figure 5 as red dashed arcs. A corner of $F_{\mathcal{C}}$ where two geodesic arcs corresponding to the reflections M_i and M_{i+1} meet at an angle of α is the center of a rotation $R_i := M_{i+1} \circ M_i$ by an angle of 2α. .

▶ **Lemma 9.** *Given a clockwise sequence of corners $c_1, ..., c_k$ of a fundamental domain $F_{\mathcal{C}}$ of a Coxeter group $*\mathsf{R}_1...\mathsf{R}_k$, the clockwise sequence of vertices of the domain F_Γ obtained by reflection across the arc from c_1 to c_k are $c_1, ..., c_k, R_k(c_{k-1}), R_k(R_{k-1}(c_{k-2})), ..., R_k(R_{k-1}(...R_3(c_2)...))$.*

The statement of the lemma is illustrated in Figure 5. The proof is deferred to Appendix D, but we offer an illustration in Figure 6, where $F_i := M_i F_{\mathcal{C}}$.

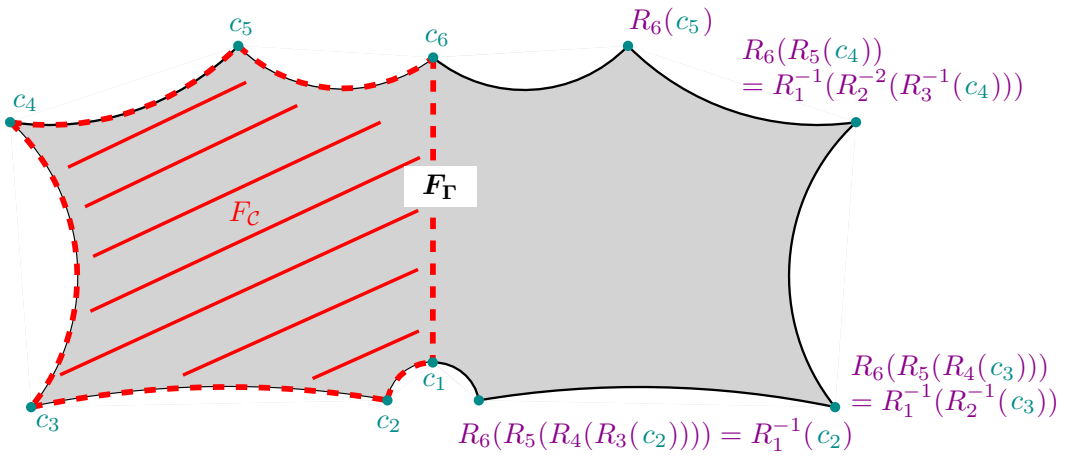

Figure 5 A fundamental domain F_Γ for a stellate group Γ generated by rotations $R_1, ..., R_6$ around the points $c_1, ..., c_6$, obtained by mirroring the fundamental domain $F_{\mathcal{C}}$ for a group generated by reflections across the dashed lines.

Proposition 10 can be considered as folklore; we give its proof in Appendix E.

▶ **Proposition 10.** *The set of rotations around corner points of a fundamental domain for $*\mathsf{R}_1...\mathsf{R}_k$ is a set of generators for $\Gamma = \mathsf{R}_1...\mathsf{R}_k$, and F_Γ is a fundamental domain for Γ.*

As a result, a natural set of starting generators would be the corners of a fundamental domain for $F_{\mathcal{C}}$ for a Coxeter supergroup. Figures 4, 7 and 8 each show an example of such a set, together with a corresponding first isotopy class of all combinatorial classes of 1-fundamental tilings.

Another useful but less general way to choose a starting set of generators for Γ comes from its characterization as a subgroup of the (the lift of) the maximal group Γ_M of symmetries of the surface S in terms of the generators of Γ_M, as described in Section 3.2. The two methods often align, but see Figure 9 for an example where this is not the case. The group is commensurate with S_D (no. 54) and isomorphic to 22222, together with a starting set of generators. Note that in contrast to the above examples, group no. 54 does not admit a Coxeter supergroup in $*246$.

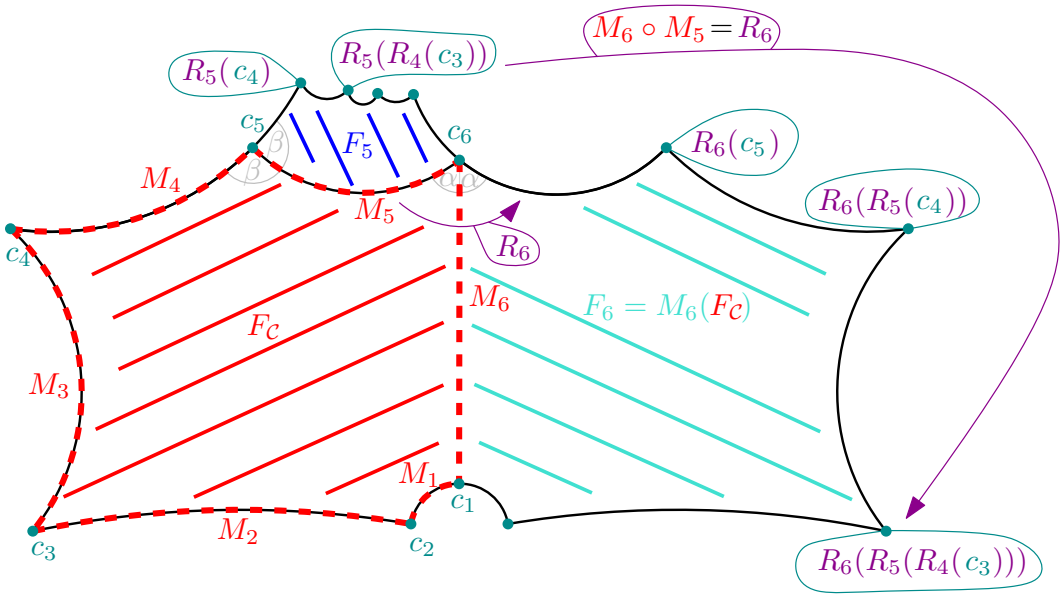

Figure 6 The expressions for the vertices of the domain F_Γ can be found inductively by applying rotations to those found in neighboring domains.

5 Computational group theory

The tools we use for the enumeration of elements of the MCG of a stellate group as well as those that we use to construct tilings are based on the underlying structure of the groups involved. It is well-known that there are finitely presented groups with undecidable word problem [8], meaning that there cannot exist an algorithm that computes a unique representative, or *normal form*, for an element of such a group in terms of a given set of generators. Since coset enumeration generalizes the enumeration of group elements, it is also undecidable in general. However, both classical MCGs and symmetry groups are automatic groups [60, 36], for which there are known algorithms that tackle the problem of finding a normal form. Note that the MCGs associated to stellate groups are finite index subgroups of classical MCGs [53, Section 5] and are thus themselves automatic [36, Section 5.6]. Moreover, although it is unknown whether the problem of coset enumeration w.r.t. finite subgroups for MCGs is solvable using available techniques, the used tools from KBMAG [35] in GAP [30] give preliminary results that allow for enumerations up to a certain word length, but are not guaranteed to yield a unique normal form for all elements. A rigorous discussion and implementations of possible extensions of available tools go beyond the scope of this paper.

For implementations, we use the only known presentation of $\mathrm{Mod}(\mathcal{O}_\Gamma)$ for stellate groups [54, Theorem 4.2], given in terms of so-called *half-twists* and *Dehn twists* [27]. These are elements of the MCG that make local changes to a surface. The resulting list (in shortlex order) somewhat captures our intuition of a complexity ordering of structures. Figure 10 shows three tilings that are separated by the application of a half-twist and its inverse. For these, the half-twist is defined as the operation that sends the first two generators R_1 and R_2 to R_2 and $R_1 \circ R_2 \circ R_1^{-1}$, respectively [54].

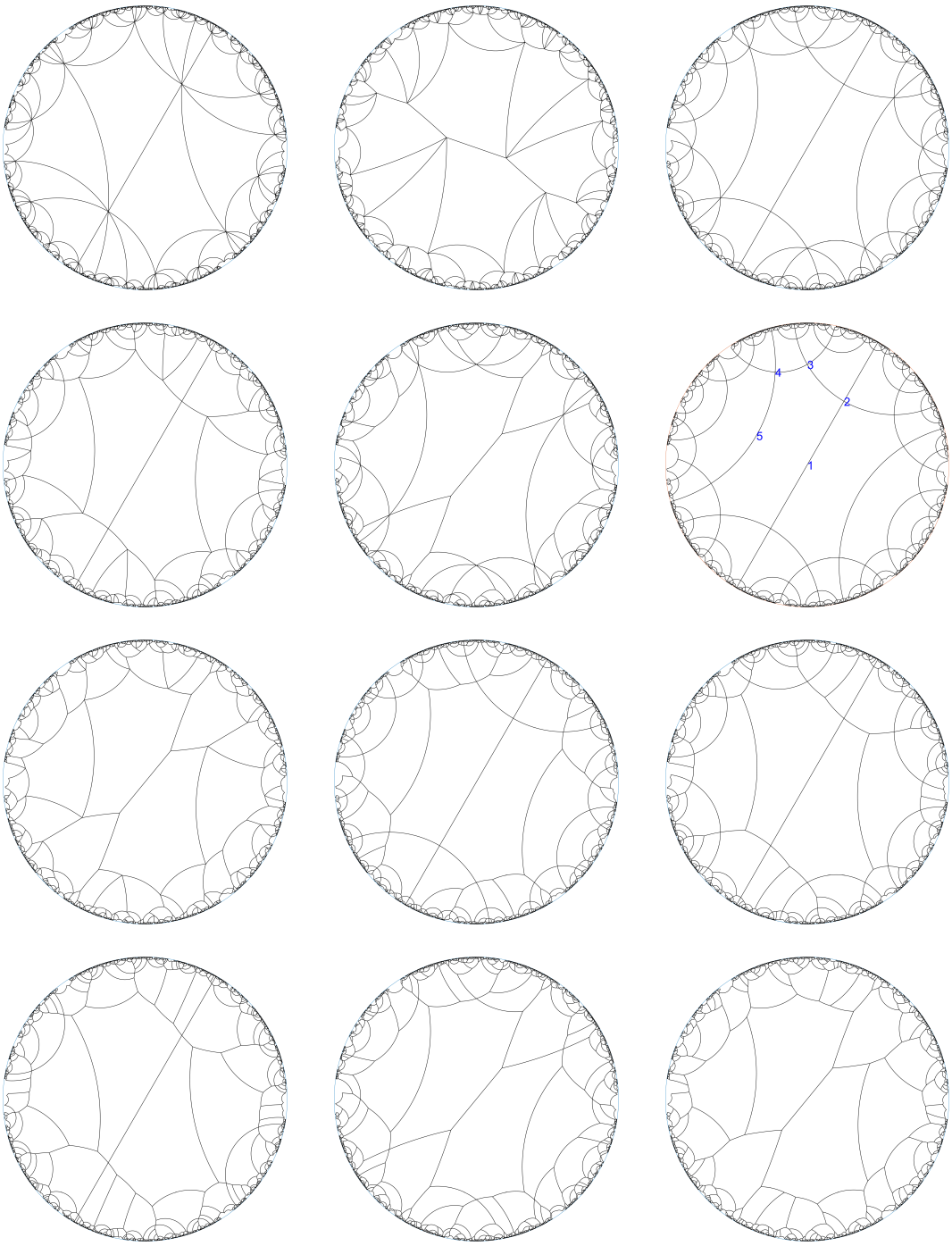

Figure 7 The different combinatorial classes of 1-fundamental tilings with symmetry group 22222 (No. 76), commensurate with the diamond TPMS. The tilings correspond to, from left to right and top to bottom, the classes QS53 to QS64 with the nomenclature from EPINET [2]. The sixth tiling shows the starting set of generators.

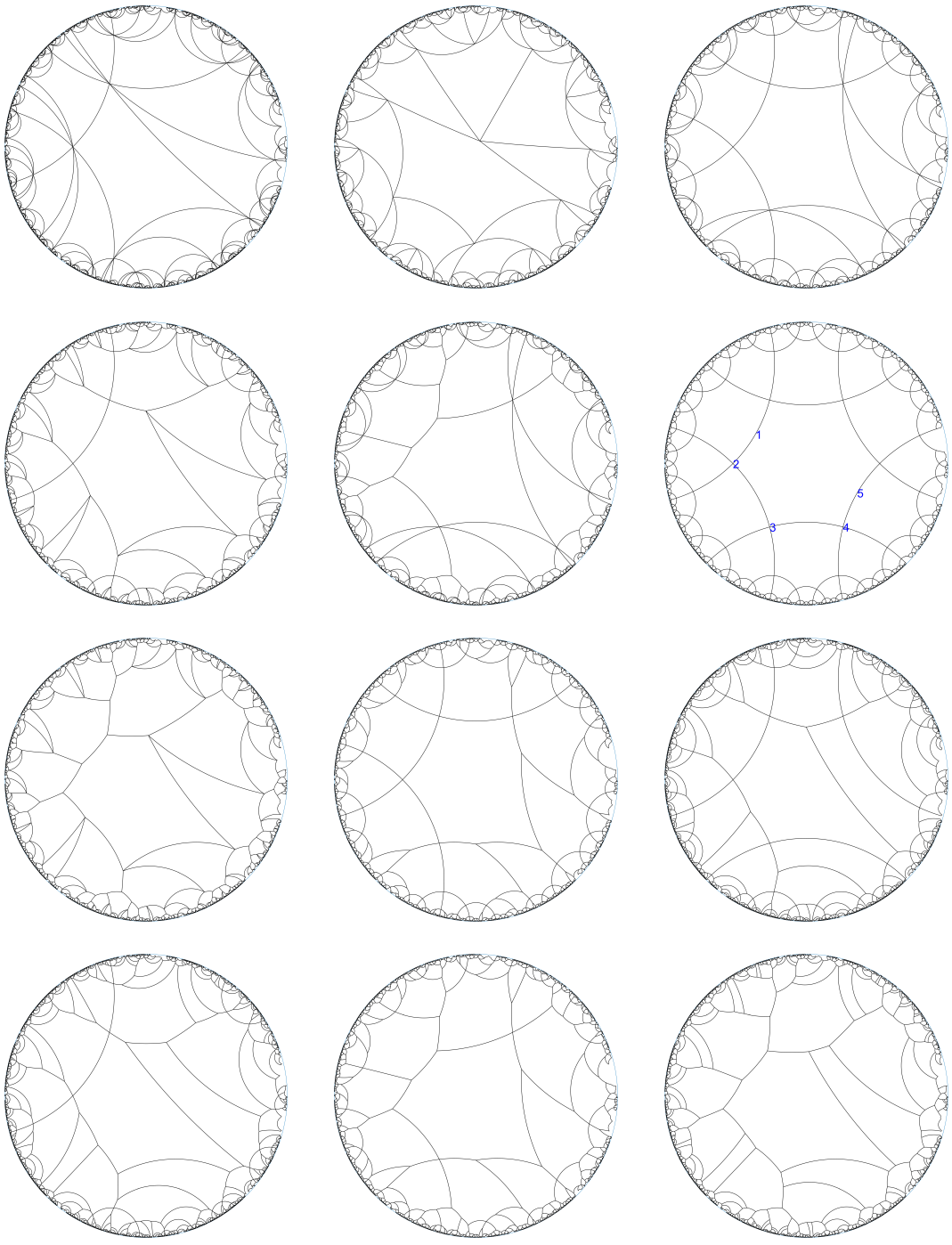

Figure 8 The same combinatorial classes of 1-fundamental tilings as in Figure 7, with symmetry group 22222 (No. 77).

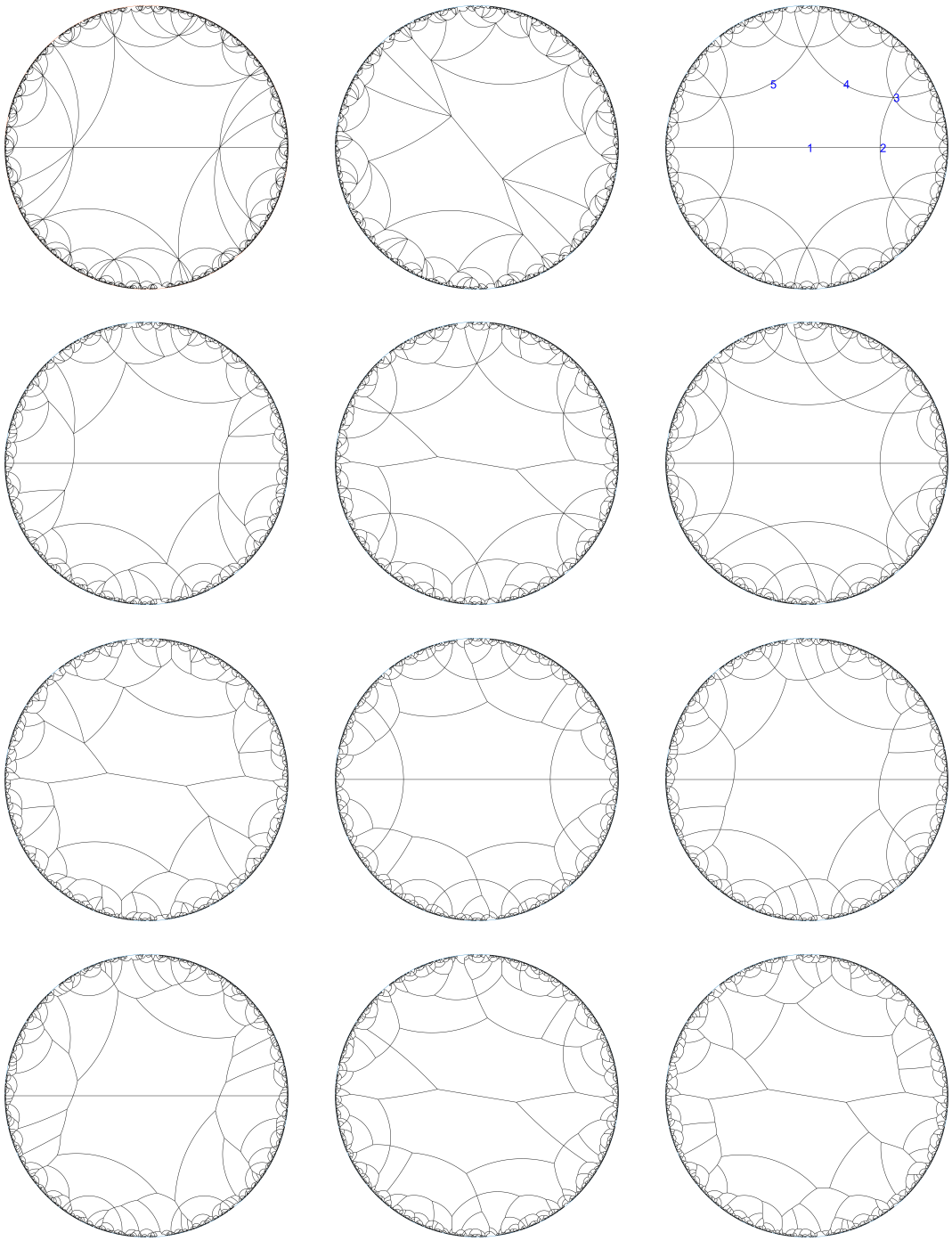

Figure 9 The same combinatorial classes of 1-fundamental tilings as in Figure 7, with symmetry group 22222 (No. 54). The third tiling shows the starting set of generators.

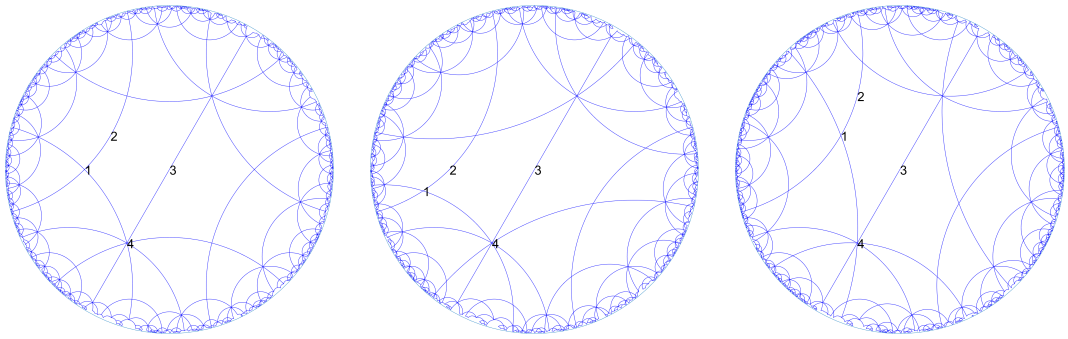

Figure 10 The effect of two mutually inverse half twists on the isotopy class of tilings with symmetry group 2224 from its action of generators. Tilings commensurate with S_D [54, Figure 9].

6 Implementations and projections to TPMS

For implementations, we simplify the problem by focusing on Algorithm 2, thereby avoiding the problem of coset enumeration by restricting to colored tilings. We briefly explain the implemented steps. First, we use the methods `KnuthBendix()` and `AutomaticStructure()` of KBMAG to generate a way to list words of both the MCG and the symmetry group. Then, using Python, we transform the list into valid input for MATLAB, which we use to generate the tilings and handle the projection to TPMS. Details on the generation, corresponding to Step 4 of Algorithm 3 can be found in Appendix G. For the projection, note that there is no parametrization of the diamond family of TPMS for the whole dodecagon, but there are known parametrizations for a given spherical triangle [28]. We convert a $*246$-triangle into a spherical $*234$ triangle using the Schwarz-Christoffel toolbox [22] and apply the symmetries in $\mathbb{H}^2$ and $\mathbb{R}^3$ appropriately to (analytically) extend the resulting parametrization on a single triangle to the whole dodecagon. The output is a graph encoded by a list L_P of points in $\mathbb{R}^3$ and another list specifying which of the points in L_P are joined by straight line segments. Creating the tilings and projecting them to the diamond TPMS with MATLAB are by far the most computationally intensive parts of the implementation.

We showcase a tiling twisted ten times (described by a word of length 10 in the MCG) in Figure 11, with symmetry group 22222. To conclude, we project this tiling and all others with symmetry group 22222 shown in this paper onto the diamond TPMS, in Figures 12, 13, 14, and 15. The 3D images were created with Houdini [69].

References

1 Epinet. Accessed: 2021-02-12. URL: `http://epinet.anu.edu.au`.

2 Epinet - fundamental domains of 22222. Accessed: 2021-02-12. URL: `http://epinet.anu.edu.au/searches/734578`.

3 Reticular chemistry structure resource. Accessed: 2021-02-12. URL: `http://rcsr.anu.edu.au/`.

4 William Abikoff. *The real analytic theory of Teichmüller space*, volume 820. 1980.

5 Lars V. Ahlfors. *Conformal invariants. Topics in geometric function theory*. AMS Chelsea Publishing, 1973.

6 J.M Alonso, T. Brady, D. Cooper, V. Ferlini, M. and Lustig, M. Mihalik, M. Shapiro, and H. Short. *Notes on word hyperbolic groups*, pages 3–63. World Scientific Publishing, 8 1991.

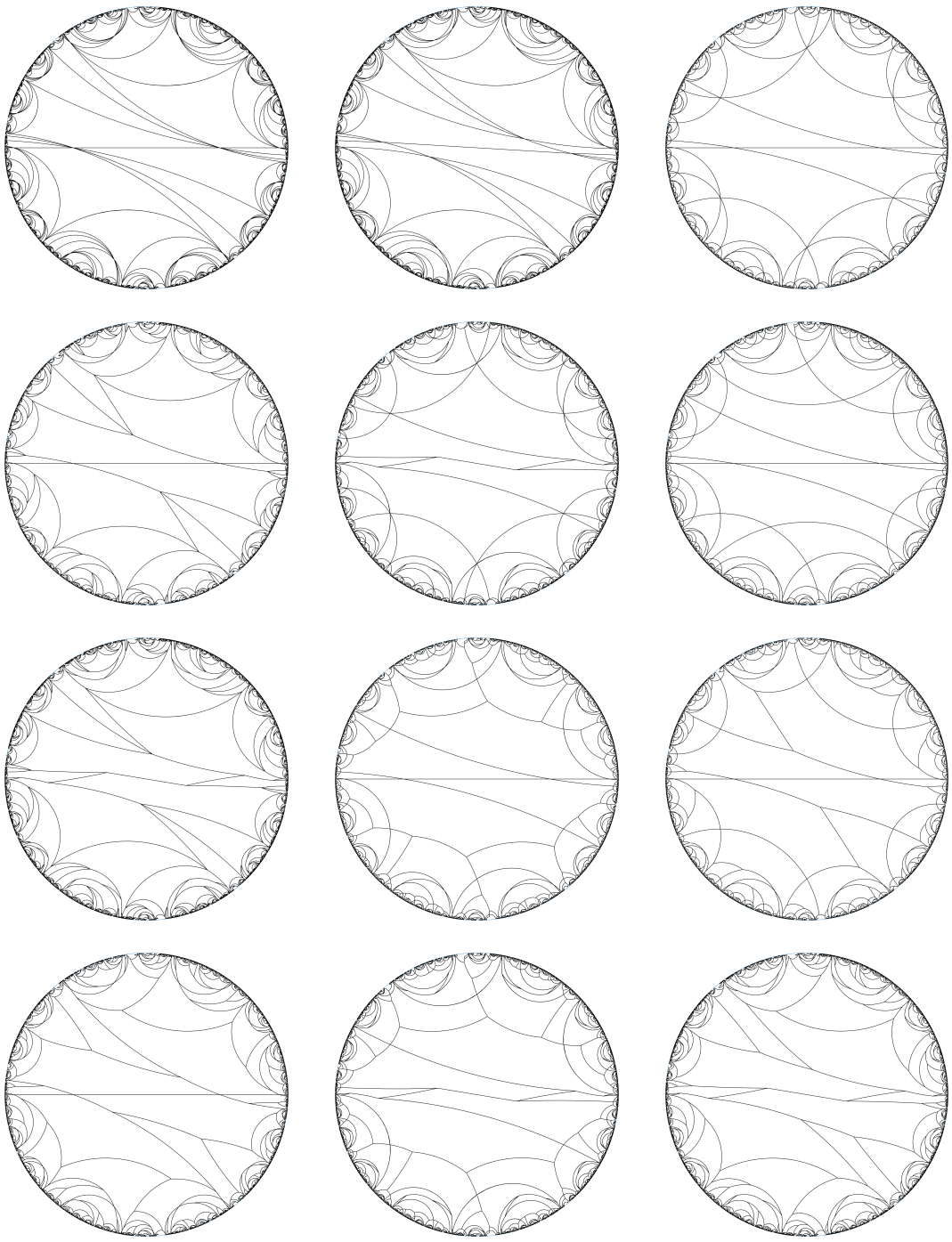

Figure 11 The different combinatorial classes of fundamental tile-1-transitive tilings with symmetry group symmetry group 22222 (No. 54). The tilings were twisted ten times.

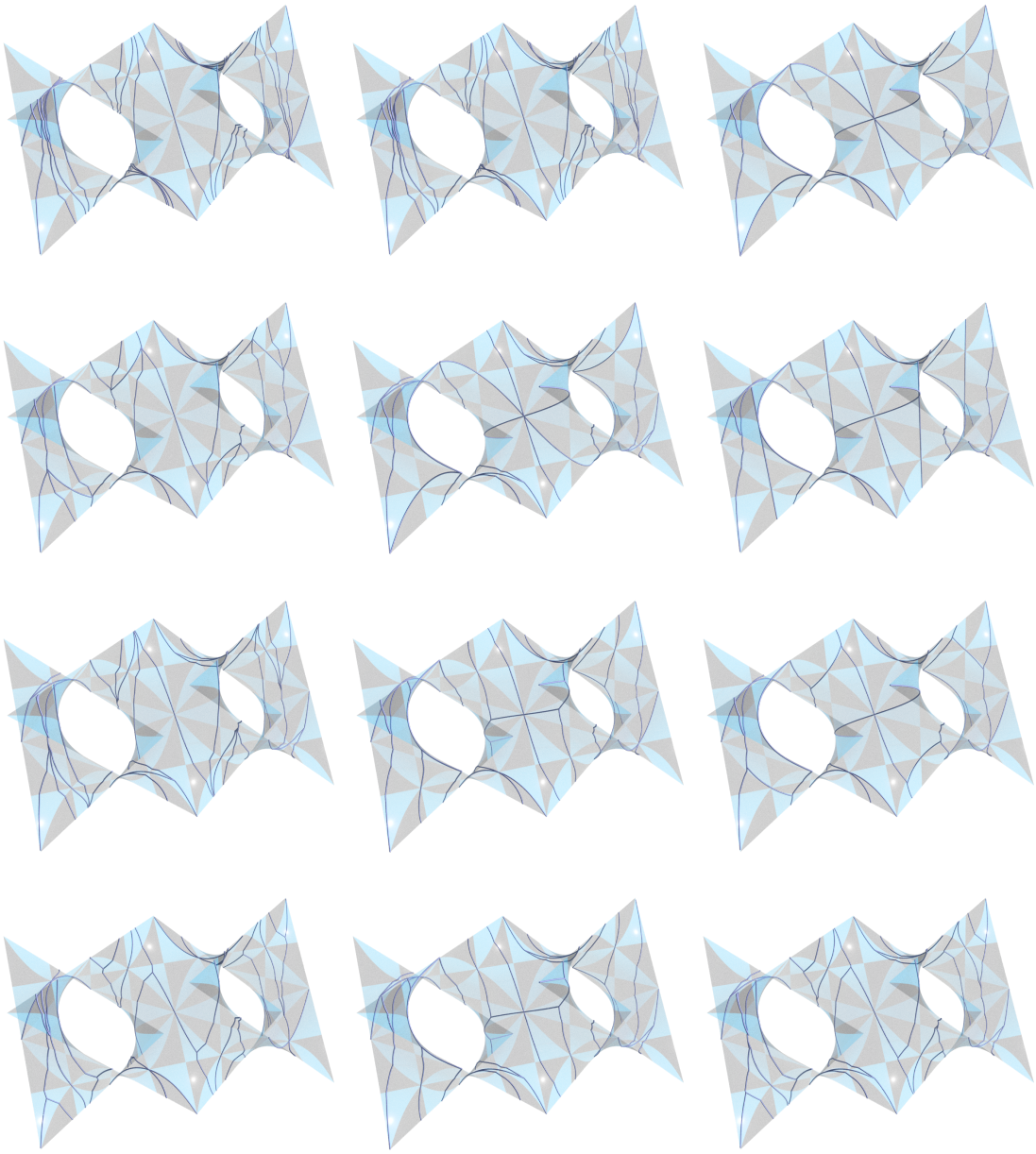

Figure 12 Nets on the diamond surface from tilings in Figure 11, with sym. group 22222 (No. 54)

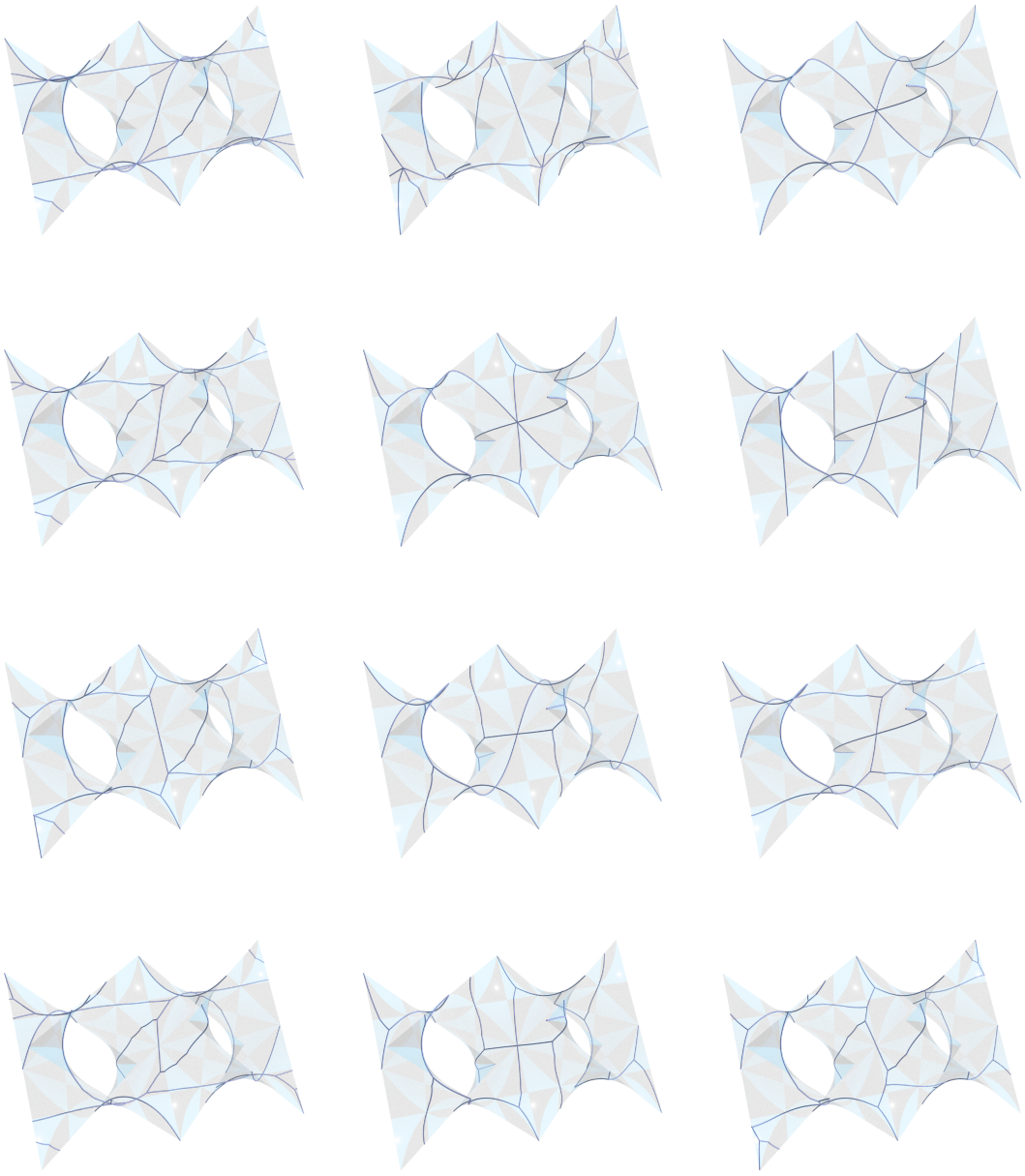

Figure 13 Nets on the diamond TPMS from tilings in Figure 9, with sym. group 22222 (No. 54).

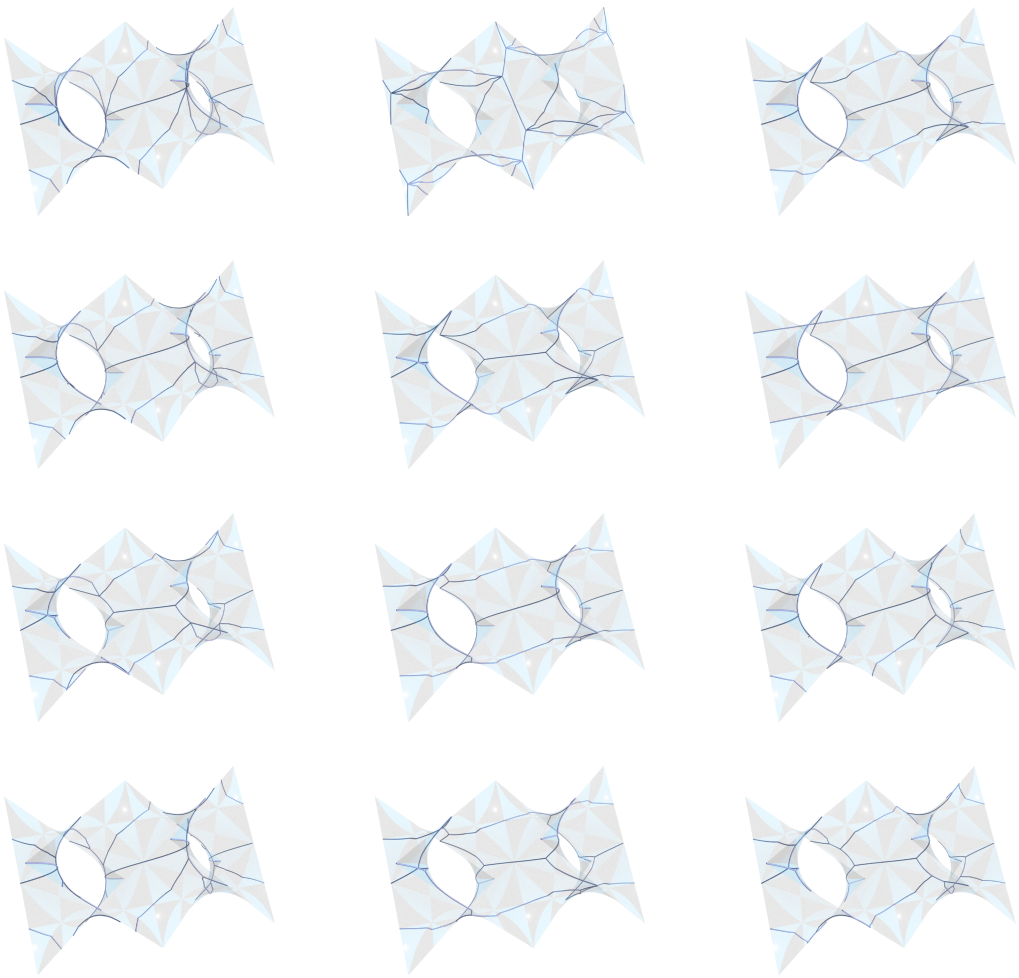

Figure 14 Nets on the diamond TPMS from tilings in Figure 7, with sym. group 22222 (No. 76).

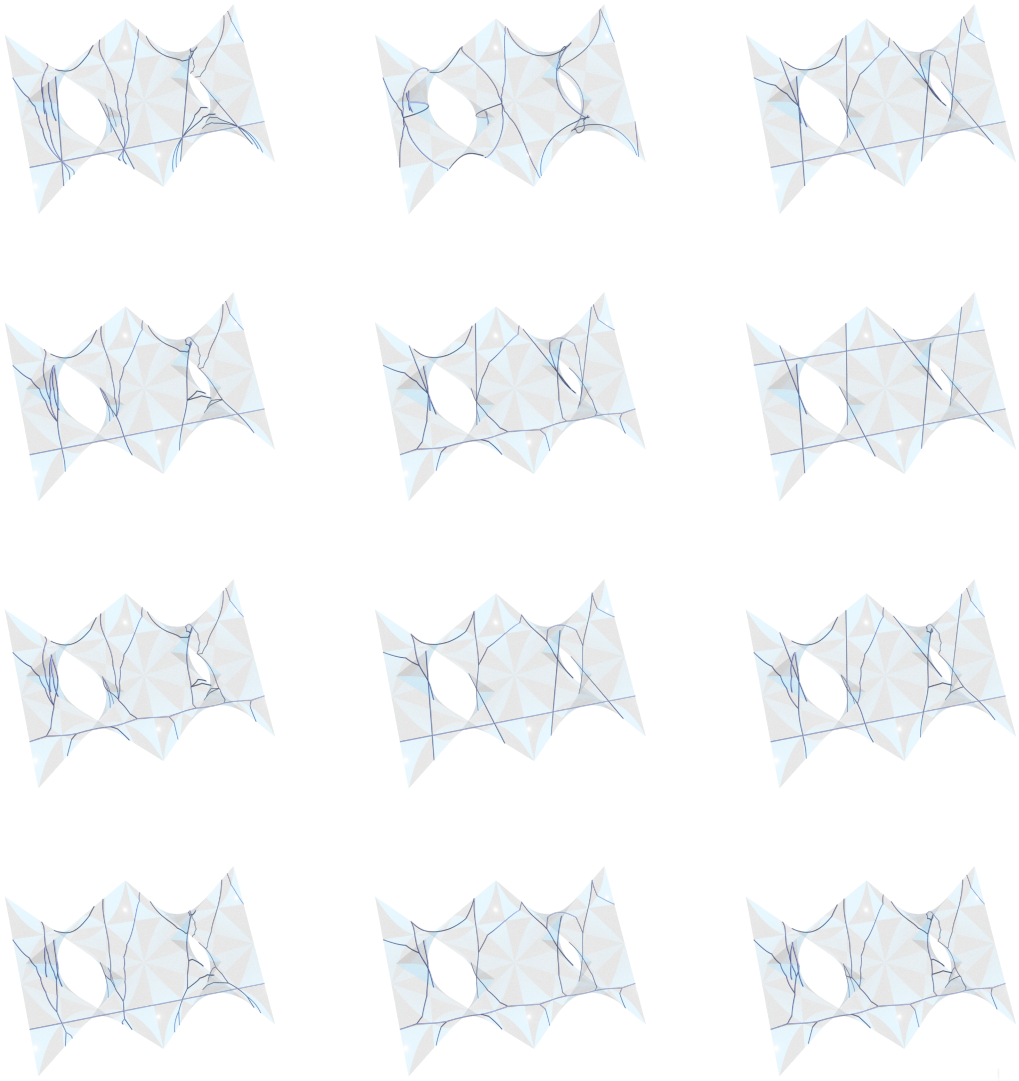

Figure 15 Nets on the diamond TPMS from tilings in Figure 8, with sym. group 22222 (No. 77).

7 Vanessa Robins Benedikt Kolbe. Tile-transitive tilings of the euclidean and hyperbolic planes by ribbons. 2020. Accepted and to appear in Research in Computational Topology 2. URL: https://hal.inria.fr/hal-03046798v1.

8 William W Boone. The word problem. *Proceedings of the National Academy of Sciences of the United States of America*, 44(10):1061–1065, 1958.

9 Svend Bundgaard and Jakob Nielsen. On normal subgroups with finite index in f - groups. *Matematisk tidsskrift. B*, pages 56–58, 1951.

10 Peter Buser. *Geometry and Spectra of Compact Riemann Surfaces*. Birkhäuser, Boston, Mass, 2nd ed. edition, 2010. doi:10.1007/978-0-8176-4992-0.

11 Toen Castle, Myfanwy E. Evans, Stephen T. Hyde, Stuart Ramsden, and Vanessa Robins. Trading spaces: building three-dimensional nets from two-dimensional tilings. *Interface Focus*, 2(January):555–66, 2012. doi:10.1098/rsfs.2011.0115.

12 T. C. Chau. A note concerning fox's paper on fenchel's conjecture. *Proc. Amer. Math. Soc.*, 88:584–586, 1983.

13 B. Chen, M. Eddaoudi, S.T. Hyde, M. O'Keeffe, and O. M. Yaghi. Interwoven metal-organic framework on a periodic minimal surface with extra-large pores. *Science*, 291:1021 – 994, 2001.

14 Y. Colin de Verdière. Comment rendre geodesique une triangulation d'une surface. *L'Enseignement Mathematique*, 37:201–212, 1991.

15 John H. Conway and Daniel H. Huson. The orbifold notation for two-dimensional groups. *Structural Chemistry*, 13(3-4):247–257, 2002. doi:10.1023/A:1015851621002.

16 Olaf Delgado-Friedrichs. Data structures and algorithms for tilings I. *Theoretical Computer Science*, 303(2-3):431–445, 2003. doi:10.1016/S0304-3975(02)00500-5.

17 Olaf Delgado-Friedrichs. Generation, analysis and visualization of reticular ornaments using gavrog, 2013. URL: http://gavrog.org/.

18 Olaf Delgado-Friedrichs and Michael O'Keeffe. Identification of and symmetry computation for crystal nets. *Acta Crystallographica Section A: Foundations of Crystallography*, 59(4):351–360, 2003. doi:10.1107/S0108767303012017.

19 Yuru Deng and Mark Mieczkowski. Three-dimensional periodic cubic membrane structure in the mitochondria of amoebae Chaos carolinensis. *Protoplasma*, 1998. doi:10.1007/BF01280583.

20 Andreas W. M. Dress and Daniel Huson. On tilings of the plane. *Geometriae Dedicata*, 24(3):295–310, Dec 1987. doi:10.1007/BF00181602.

21 Andreas W.M Dress. Presentations of discrete groups, acting on simply connected manifolds, in terms of parametrized systems of coxeter matrices-a systematic approach. *Advances in Mathematics*, 63(2):196 – 212, 1987. doi:https://doi.org/10.1016/0001-8708(87)90053-3.

22 T. A. Driscoll. A matlab toolbox for schwarz–christoffel mappings, 1996. Accessed: 2021-02-12. URL: https://de.mathworks.com/matlabcentral/fileexchange/1316-schwarz-christoffel-toolbox.

23 Myfanwy E. Evans and Stephen T. Hyde. Periodic entanglement III: tangled degree-3 finite and layer net intergrowths from rare forests. *Acta Crystallographica Section A*, 71(6):599–611, Nov 2015. doi:10.1107/S2053273315014710.

24 Myfanwy E. Evans, Vanessa Robins, and Stephen T. Hyde. Periodic entanglement i: networks from hyperbolic reticulations. *Acta Crystallographica Section A*, 69(3):241–261, 2013. doi:10.1107/S0108767313001670.

25 Myfanwy E. Evans, Vanessa Robins, and Stephen T. Hyde. Periodic entanglement II: weavings from hyperbolic line patterns. *Acta Crystallographica Section A*, 69(3):262–275, 2013. doi:10.1107/S0108767313001682.

26 Myfanwy E. Evans, Vanessa Robins, and Stephen T. Hyde. Ideal geometry of periodic entanglements. In *Proceedings of the Royal Society A: Mathematical, Physical and Engineering Sciences*, 2015. doi:10.1098/rspa.2015.0254.

27 Benson Farb and Dan Margalit. *A Primer on Mapping Class Groups (PMS-49)*. Princeton University Press, 2012. URL: http://www.jstor.org/stable/j.ctt7rkjw.

28 A. Fogden and S. T. Hyde. Parametrization of triply periodic minimal surfaces. II. regular class solutions. *Acta Crystallographica Section A: Foundations of Crystallography*, 48(4):575–591, 1992. doi:10.1107/S0108767392002885.

29 Ralph H. Fox. On fenchel's conjecture about f-groups. *Matematisk Tidsskrift. B*, pages 61–65, 1952. URL: http://www.jstor.org/stable/24530069.

30 The GAP Group. *GAP – Groups, Algorithms, and Programming, Version 4.11.0*, 2020.

31 Karsten Große-Brauckmann and Wohlgemuth Meinhard. The gyroid is embedded and has constant mean curvature companions. *Calculus of Variations and Partial Differential Equations*, 4(6):499–523, Oct 1996. doi:10.1007/BF01261761.

32 Allen Hatcher. *Algebraic topology*. Cambridge University Press, 2002.

33 John Hempel. Residual finiteness of surface groups. *Proc. Amer. Math. Soc.*, 32(1), 1972.

34 I. N. Herstein. *Topics in Algebra*. John Wiley & Sons, 2 edition, 1975.

35 Derek Holt. The knuth-bendix program on semigroups, monoids and groups. Accessed: 2021-02-12. URL: https://www.gap-system.org/Packages/kbmag.html.

36 Derek Holt, Sarah Rees, and Claas Rover. *Groups, Languages and Automata*. Cambridge University Press, 2017.

37 Daniel H. Huson. The generation and classification of tile-k-transitive tilings of the euclidean plane, the sphere and the hyperbolic plane. *Geometriae Dedicata*, 47(3):269–296, Sep 1993. doi:10.1007/BF01263661.

38 S. Hyde and S. Ramsden. Chemical frameworks and hyperbolic tilings. In P. Hansen, P. Fowler, and M. Zheng, editors, *Discrete Mathematical Chemistry*, pages 203–224. American Mathematical Society, 2000. doi:10.1090/dimacs/051/15.

39 S. T. Hyde. Hyperbolic surfaces in the solid-state and the structure of ZSM–5 zeolites. *Acta Chem Scand*, 45:860 – 863, 1991.

40 S. T. Hyde. Crystalline frameworks as hyperbolic films. In J.N. Boland and J. D. FitzGerald, editors, *Defects and processes in the solid state: Geoscience applications*. Elsevier, Amsterdam, 1993.

41 S. T. Hyde and S. Andersson. A systematic net description of saddle polyhedra and periodic minimal surfaces. *Z Kristallogr*, 168:221 – 254, 1984.

42 S. T. Hyde, O. Delgado Friedrichs, S. J. Ramsden, and V. Robins. Towards enumeration of crystalline frameworks: the 2D hyperbolic approach. *Solid State Sci*, 8:740 – 752, 2006.

43 S. T. Hyde and C. Oguey. From 2D hyperbolic forests to 3D Euclidean entangled thickets. *European Physical Journal B*, 16(4):613–630, 2000. doi:10.1007/PL00011063.

44 S. T. Hyde and S. Ramsden. Polycontinuous morphologies and interwoven helical networks. *EPL (Europhysics Letters)*, 50(2):135, 2000. URL: http://stacks.iop.org/0295-5075/50/i=2/a=135.

45 S. T. Hyde, S. Ramsden, T. Di Matteo, and J. J. Longdell. Ab-initio construction of some crystalline 3D Euclidean networks. *Solid State Sciences*, 5(1):35–45, 2003. doi:10.1016/S1293-2558(02)00079-1.

46 S. T. Hyde and S. J. Ramsden. Some novel three-dimensional euclidean crystalline networks derived from two-dimensional hyperbolic tilings. *Eur Phys J B*, 31:273 – 284, 2003.

47 Stephen T. Hyde and Martin Cramer Pedersen. Schwarzite nets: a wealth of 3-valent examples sharing similar topologies and symmetries. *Proceedings of the Royal Society A*, 477(2246), feb 2021. URL: https://royalsocietypublishing.org/doi/abs/10.1098/rspa.2020.0372, doi:10.1098/RSPA.2020.0372.

48 Stephen T Hyde, T Landh, S Lidin, B W Ninham, K Larsson, and S Andersson. *The Language of Shape*. Elsevier Science, 1996.

49 Stephen T. Hyde, Ann Kristin Larsson, Tiziana Di Matteo, Stuart Ramsden, and Vanessa Robins. Meditation on an Engraving of Fricke and Klein (The Modular Group and Geometrical Chemistry). In *Australian Journal of Chemistry*, 2003. doi:10.1071/CH03191.

50 Iordan Iordanov and Monique Teillaud. 2D periodic hyperbolic triangulations. In *CGAL User and Reference Manual*. CGAL Editorial Board, 5.1 edition, 2020. URL: https://doc.cgal.org/5.1/Manual/packages.html#PkgPeriodic4HyperbolicTriangulation2.

51 Sebastian C. Kapfer, Stephen T. Hyde, Klaus Mecke, Christoph H. Arns, and Gerd E. Schröder-Turk. Minimal surface scaffold designs for tissue engineering. *Biomaterials*, 32(29):6875–6882, 2011. doi:10.1016/j.biomaterials.2011.06.012.

52 Jacob J K Kirkensgaard, Myfanwy E Evans, Liliana de Campo, and Stephen T Hyde. Hierarchical self-assembly of a striped gyroid formed by threaded chiral mesoscale networks. *Proceedings of the National Academy of Sciences of the United States of America*, 111(4):1271–6, 2014. URL: http://www.pnas.org/cgi/content/long/111/4/1271, doi:10.1073/pnas.1316348111.

53 Benedikt Kolbe and Myfanwy Evans. Isotopic tiling theory for hyperbolic surfaces. *Geometriae Dedicata*, 2020. doi:10.1007/s10711-020-00554-2.

54 Benedikt Kolbe and Myfanwy Evans. Enumerating isotopy classes of tilings guided by the symmetry of triply-periodic minimal surfaces. 2021. Accepted and to appear in: SIAM Journal on Applied Algebra and Geometry (SIAGA). URL: https://arxiv.org/abs/1808.00984.

55 Benedikt Maximilian Kolbe. *Structures in three-dimensional Euclidean space from hyperbolic tilings*. Doctoral thesis, Technische Universität Berlin, Berlin, 2020. URL: http://dx.doi.org/10.14279/depositonce-10476, doi:10.14279/depositonce-10476.

56 Murasugi Kunio. Seifert fibre spaces and braid groups. *Proceedings of the London Mathematical Society*, 44(1):71–84, 1982. doi:10.1112/plms/s3-44.1.71.

57 Z. Lučić and E. Molnár. Fundamental domains for planar discontinuous groups and uniform tilings. *Geometriae Dedicata*, 40(2):125–143, Nov 1991. doi:10.1007/BF00145910.

58 A. M. Macbeath. The classification of non-euclidean plane crystallographic groups. *Canadian Journal of Mathematics*, 19:1192–1205, 1967. URL: http://www.cms.math.ca/10.4153/CJM-1967-108-5, doi:10.4153/CJM-1967-108-5.

59 Meeks. The Theory of Triply Periodic Minimal Surfaces, 1990. doi:10.1512/iumj.1990.39.39043.

60 Lee Mosher. Mapping Class Groups are Automatic. *Annals of Mathematics*, 142(2):303–384, 1995. URL: https://www.jstor.org/stable/2118637.

61 Gou Nakamura and Toshihiro Nakanishi. Generation of finite subgroups of the mapping class group of genus 2 surface by Dehn twists. *Journal of Pure and Applied Algebra*, 222(11):3585–3594, nov 2018. doi:10.1016/J.JPAA.2018.01.002.

62 Reinhard Nesper and Stefano Leoni. On tilings and patterns on hyperbolic surfaces and their relation to structural chemistry. *ChemPhysChem*, 2(7):413–422, 2001. doi:10.1002/1439-7641(20010716)2:7<413::AID-CPHC413>3.0.CO;2-V.

63 Martin Cramer Pedersen, Olaf Delgado-friedrichs, and Stephen T Hyde. Surface embeddings of the Klein and the Mobius – Kantor graphs. *Acta Crystallographica Section A*, 74:223–232, 2018. doi:10.1107/S2053273318002036.

64 Martin Cramer Pedersen and Stephen T. Hyde. Polyhedra and packings from hyperbolic honeycombs. *Proceedings of the National Academy of Sciences of the United States of America*, 2018. doi:10.1073/pnas.1720307115.

65 Joaquín Pérez and Antonio Ros. *Properly embedded minimal surfaces with finite total curvature*, pages 15–66. Springer Berlin Heidelberg, Berlin, Heidelberg, 2002. doi:10.1007/978-3-540-45609-4_2.

66 S. J. Ramsden, V. Robins, and S. T. Hyde. Three-dimensional Euclidean nets from two-dimensional hyperbolic tilings: kaleidoscopic examples. *Acta Crystallographica Section A*, 65(2):81–108, Mar 2009. doi:10.1107/S0108767308040592.

67 V Robins, S J Ramsden, and S T Hyde. 2D hyperbolic groups induce three-periodic Euclidean reticulations. *The European Physical Journal B*, 39(3):365–375, 2004. doi:10.1140/epjb/e2004-00202-2.

68 J. -F Sadoc and J. Charvolin. Infinite periodic minimal surfaces and their crystallography in the hyperbolic plane. *Acta Crystallographica Section A*, 45(1):10–20, 1989. doi:10.1107/S0108767388008438.

69 SideFX. Houdini sidefx software. URL: https://www.sidefx.com/.

70 William Thurston. *Geometry and Topology of Three-Manifolds*. Princeton lecture notes, 1980.

71 Dierkes Ulrich, Stefan Hildebrandt, and Friedrich Sauvigny. *Minimal Surfaces*. Springer-Verlag Berlin Heidelberg, 2 edition, 2010.

72 Adam G. Weyhaupt. Deformations of the gyroid and Lidinoid minimal surfaces. *Pacific J. Math.*, 235(1):137–171, 2008.

73 A. Williams. Maf (monoid automata factory)„ 2009. Accessed: 2021-02-12. URL: http://maffsa.sourceforge.net/.

74 Henry Wilton. Mapping class groups (lecture notes), 2021. URL: https://www.dpmms.cam.ac.uk/~hjrw2/MCG%20lectures.pdf.

75 Bodo D. Wilts, Benjamin Apeleo Zubiri, Michael A. Klatt, Benjamin Butz, Michael G. Fischer, Stephen T. Kelly, Erdmann Spiecker, Ullrich Steiner, and Gerd E. Schroeder-Turk. Butterfly gyroid nanostructures as a time-frozen glimpse of intracellular membrane development. *Science Advances*, 3(4), 4 2017.

76 Rüdiger Zeller, Olaf Delgado-Friedrichs, and Daniel H. Huson. Tegula – exploring a galaxy of two-dimensional periodic tilings. *Computer Aided Geometric Design*, 90:102027, oct 2021. arXiv:2007.10625, doi:10.1016/J.CAGD.2021.102027.

A Orbifolds

In the literature, a symmetry group Γ of $\mathbb{H}^2$, i.e. a discrete group of isometries of $\mathbb{H}^2$ having a compact fundamental domain is known as a NEC group (non-Euclidean crystallographic group). We identify the isomorphism class of a group using Conway's *orbifold symbol* [15], a highly-readable version of Macbeath's group signature [58], as described below.

For the purposes of this paper an (2-)orbifold, $\mathcal{O}_\Gamma$, is a quotient space $\mathbb{H}^2/\Gamma$ obtained by identifying points of $\mathbb{H}^2$ that are equivalent under the action of Γ, i.e. $x \sim y$ if $y = \gamma x$ for some $\gamma \in \Gamma$. The quotient space can be endowed with the quotient topology.

The difference between $\mathbb{H}^2/\Gamma$ as a topological space and as an orbifold is that the full orbifold structure retains the metric information carried by the particular isometries of Γ and an atlas of charts compatible with the Γ action. We require both the topological view point and orbifold structure of the quotient space, and will use the script notation $\mathcal{O}_\Gamma$ for the orbifold with the additional structure and plain O_Γ for its underlying topological space.

We say that $\mathcal{O}_{\Gamma_1} \to \mathcal{O}_{\Gamma_2}$ is an n-fold covering of orbifolds if $\Gamma_1 \subset \Gamma_2$ is an index n subgroup [70, Chapter 13].

It is well-known [70] that 2-orbifolds are topologically equivalent to compact 2-manifolds with a finite number of boundary components and marked points. Boundaries in a 2-orbifold arise from the fixed lines of reflection isometries while marked points arise as the fixed points of rotational isometries. The marked points are called *cone points* if they lie in the interior of the orbifold, and *corner points* if they lie on a boundary. The order, N, of a cone or corner point is the order of the rotational isometry, σ, that fixes that point i.e. $\sigma^N = id$. The boundaries and marked points are collectively referred to as the *singular locus* of the orbifold. The topology of a 2-orbifold (O) is therefore specified by a symbol as follows:

1. The number of handles, h, if the orbifold is orientable, or the number of cross-caps, k, if non-orientable. Handles are denoted by $\circ$ at the beginning of the orbifold symbol. Cross-caps are denoted by $\times$ at the end of the orbifold symbol.
2. The order for each cone point, listed in arbitrary order after any handles.

3. The number of boundary components, q. Each boundary component is represented by a $*$ in the symbol. Branching numbers for the corner points lying on each boundary component are listed in cyclic order, such that each boundary component has a consistent orientation for the manifold. The ordering of the boundary components is arbitrary.

Simple examples include the group of isometries for a square tiling of $\mathbb{E}^2$, which is $*\mathsf{244}$ ($p4m$ in Hermann-Mauguin notation). Note that for a Euclidean pattern with only translational symmetries the same example has the symmetry group $\circ$ ($p1$).

It is well-known [70, 15] that any orbifold symbol corresponds to a discrete group of isometries of $\mathbb{E}^2$, $\mathbb{H}^2$, or $\mathbb{S}^2$, with the exception of the symbols A, $*\mathsf{A}$, AB, and $*\mathsf{AB}$, with $\mathsf{A} \neq \mathsf{B}$. The Conway orbifold symbol is useful mainly for the following reasons: it allows the computation of the orbifold Euler characteristic, which determines the plane geometry associated with an orbifold, as an orbifold is hyperbolic if its orbifold Euler characteristic is negative [15]. The absolute value of the Euler characteristic of a symmetry group corresponds to its area. Furthermore, a well-known fact states that symmetry groups with the same symbol give rise to topologically equivalent realizations as symmetry groups [58]. This implies, in particular, that if a symmetry group with Conway symbol CS_1 has a subgroup with CS_2, then any symmetry group with symbol CS_1 has a subgroup with symbol CS_2.

B Proof of Proposition 1

Proof. Assume on the contrary that there was an embedding of a graph G onto S that lifts to the edge graph $\tilde{G}$ of $\mathcal{T}$ in $\mathbb{H}^2$ for which $S \setminus G$ had a component C that is not a disk. Note first that G must be connected since the edge graph of $\mathcal{T}$ is connected. Let c be a noncontractible simple loop in C. Then c cannot be contractible in S because G is connected. It is well-known that a noncontractible curve on the closed surface $\pi_1(S)$ corresponds to a nontrivial hyperbolic translation in $\mathbb{H}^2$ [4, p. 4, Lemma 1]. Denote by $\tilde{c}$ a connected component of the union of all lifts to $\mathbb{H}^2$ of c and observe that in the Poincaré disk model $\tilde{c}$ connects two points of the boundary of the disk. Now, $\tilde{c}$ is entirely contained in a component of $\mathbb{H}^2 \setminus \tilde{G}$ and $\mathbb{H}^2 \setminus \tilde{c}$ has two components, which contradicts the assumption that each tile in $\mathcal{T}$ is a compact disk. ◀

C Lifts to the oriented double cover

▶ **Lemma 11.** *Let f be a homeomorphism of an orbifold $\mathcal{N}$ with nonorientable quotient space. Then there is a lift $\tilde{f}$ of f to a homeomorphism of the oriented double cover $\mathcal{O}$ that is moreover orientation preserving.*

Proof. We sketch the proof. Denote by p the projection from $\mathcal{O}_{\Gamma^+}$ to $\mathcal{O}_\Gamma$. Outside the singular locus Σ (a nowhere dense set of measure zero), p is a usual covering map, so if we ignore Σ, then $f \circ p$ lifts to a map $\tilde{f} : \mathcal{O}_{\Gamma^+} \to \mathcal{O}_{\Gamma^+}$ iff $(f \circ p)_*(\pi_1(\mathcal{O})) \subset p_*(\mathcal{O})$ [32, Prop. 1.33]. Now, $p_*(\mathcal{O})$ consists of loops that lift to loops in $\mathcal{O}$ [32, Prop. 1.31], i.e. two-sided loops in $\mathcal{N}$ that do not change the local orientation in a neighborhood, or, in other words, loops which admit a neighborhood that is an annulus. Since annuli are preserved by f, f_* maps such loops to themselves. Therefore, there exists a lift $\tilde{f}$ of f. One simialrly sees that $\tilde{f}$ is in fact a homeomorphism. Since any index 2 subgroup is normal, the covering is regular, i.e. there exists a homeomorphism $r : \mathcal{O} \to \mathcal{O}$ that exchanges the two sheets (orientations) of the oriented double cover, s.t. $p \circ r = r \circ p$. Precomposing or postcomposing $\tilde{f}$ with r yields another lift of f, so we can assume that $\tilde{f}$ preserves the orientation of $\mathcal{O}$. ◀

D Proof of Proposition 9

Proof. To begin with, we observe that if the statement holds with the given ordering of the edges, then similar statements hold in case one reflects $F_{\mathcal{C}}$ across a different boundary arc. Using this observation, we prove the statement by induction. It is clear that the first vertex in clockwise direction after c_k is given by $R_k(c_{k-1})$, since $R_k = M_k M_{k-1}$, so we can assume that the expression given in the statement of the lemma holds for the first $l-1$ vertices of encountered along F_Γ. By the above observation, the first $l-1$ vertices encountered when traveling around the boundary of F_{k-1} clockwise are then given by the sought-for expressions, as illustrated in Figure 6. Now, $R_k(D) = M_k(M_{k-1}(D)) = M_k(F_{\mathcal{C}}) = F_k$, so, since R_k is orientation preserving, it maps the l-th vertex in F_{k-1} to the l-th vertex in F_k, both counted clockwise from c_k, thereby proving the induction step. ◀

E Proof of Proposition 10

Proof. For the proof, it is sufficient to show that F_Γ serves as a fundamental domain for the group R generated by the rotations $R_1, ..., R_k$. Since F_Γ has twice the area of $F_{\mathcal{C}}$, the group generated by these rotations then has Conway notation $\mathsf{R_1...R_k}$ (i.e. all rotations are necessary). Lemma 9 implies that the set of all corner points of copies of F_Γ under R are centers of rotation in R. Furthermore, every edge of a copy of F_Γ in RF_Γ is incident to two copies of F_Γ. To see this, it is enough to show this for F_Γ, see Figure 6. For F_Γ, observe that whenever F_i is incident to a vertex c_{i+1} such that F_{i+1} is covered by a copy of F_k, then $F_i = R_{i+1}^{-1}(F_{i+1})$. We similarly deduce that all edges of F_Γ incident to F_k are covered by copies, under R, of $F_{\mathcal{C}}$. Since no rotations in $*\mathsf{R_1...R_k}$ have centers anywhere but on the corners of copies of $F_{\mathcal{C}}$, the group R contains all rotations contained in $*\mathsf{R_1...R_k}$ and thus F_Γ constitutes a fundamental domain for $R = \mathsf{R_1...R_k}$. ◀

F Proof of Theorem 8

Proof. We first show that for a cellular embedding of a graph G' on a hyperbolic surface S', there is a finite sheeted covering surface where the lifted graph has the property that barycentric subdivision on each face yields a simplicial complex. To see this, we use that $\pi_1(S')$ is residually finite [33], which means that for any $\alpha \in \pi_1(S')$, there is a finite index normal subgroup $\mathcal{N}_\alpha \subset \pi_1(S')$ that does not contain α. Thus, if $\{\alpha_i\}_{i=1}^k$ is a finite list of all closed geodesics of length $\leq L \in \mathbb{R}$ [10, Theorem 1.6.11], $\mathcal{N} := \bigcap_i \mathcal{N}_{\alpha_i}$ is a finite index normal subgroup of $\pi_1(S')$ that does not contain any of the α_i. Here we use the interpretation of $\pi_1(S)$ as homotopy classes of closed curves [32]. The group $\mathcal{N}$ corresponds to the group of covering transformations of a finite sheeted locally isometric covering of S' by a hyperbolic surface S. By construction, S does not contain any closed geodesics of length $\leq L$.

A simplicial complex is a characterized by the property that it is a triangulation and that the smallest edge cycles are of length at least 3. We can turn G' into a triangulation by (topological) barycentric subdivision, so we can assume for simplicity that G represents the edges of a triangulation of S' (though not necessarily a simplicial complex). Each edge of G' has a geodesic in its homotopy class with fixed endpoints, which minimizes the length of all curves in the same homotopy class connecting these endpoints [10, Theorem 1.5.3]. Let l be the length of the longest geodesic representative of the edges in G. Then the surface S contructed above with $L = 3l$ along with the lift G of G' has the sought-for properties, since the smallest cycle has length at least 3, by construction.

It is known that there exists a finite index subgroup of Γ that is the fundamental group of a closed hyperbolic surface S [29, 9, 12]. One can further assume that $\pi_1(S) \subset \Gamma$ is normal, by passing to a finite index subgroup [34, p. 48], which corresponds to a finite covering space of the closed surface and is therefore also a closed surface.

Thus, there exists a finite covering surface S of the orbifold $\mathcal{O}_\Gamma$ such that G_S is invariant under the action of the group of isometries $I := \Gamma/\pi_1(S)$ on S. Moreover, by Proposition 1, the edges of $\mathcal{T}$ project onto a graph G on $\mathcal{O}_\Gamma$ such that the graph G_S obtained from lifting G to S is a cellular embedding. We can further assume that the edges of G_S are a subgraph of the 1-skeleton of a simplicial complex in S by the above. Now, any simplicial complex embedded on a closed hyperbolic surface is isotopic to an embedding with only geodesic edges [14], so we can turn G_S into a graph G'_S with geodesic edges by using an isotopy of S. Moreover, in [14], G'_S is obtained as a minimizer of a functional that depends only on the metric and G_S, the embedding of the graph one started off with. Since both of these are invariant under I, G'_S is also invariant under I. Therefore, $(\mathcal{T}', \Gamma)$ is an equivariant tiling, where $\mathcal{T}'$ denotes the lift of G'_S to $\mathbb{H}^2$. Since G_S to G'_S are isotopic on S, $(\mathcal{T}, \pi_1(S))$ and $(\mathcal{T}', \pi_1(S))$ have isomorphic D-symbols.

For a given equivariant equivalence class $(\mathcal{T}, H)$, there is a unique equivariant equivalence class $(\hat{\mathcal{T}}, \Gamma_M)$, where $\Gamma_M \supset H$ is the maximal symmetry group of the topological equivalence class of the tiling $\mathcal{T}$ [18, p. 438]. Thus, there is a representative $(\hat{\mathcal{T}}, \Gamma_M)$ with maximal symmetry group Γ_M. This implies that $(\mathcal{T}, \Gamma)$ and $(\mathcal{T}', \Gamma)$ are equivariantly equivalent, since $\Gamma \subset \Gamma_M$.

The equivariant equivalence of $(\mathcal{T}, \Gamma)$ and $(\mathcal{T}', \Gamma)$ implies, in particular, that both tilings are fundamental tile-1-transitive. Therefore, the lifted isotopy between G_S to G'_S to $\mathbb{H}^2$ to obtain an isotopy between $\mathcal{T}$ and $\mathcal{T}'$ gives rise to a Γ-equivariant homeomorphism φ mapping $\mathcal{T}$ to $\mathcal{T}'$. By construction, φ is isotopic to the identity map via a path of $\pi_1(S)$-equivariant homeomorphisms. Such a homeomorphism is in fact isotopic to the identity map via a path of Γ-equivariant homeomorphisms [53, Proposition 3], so $(\mathcal{T}', \Gamma)$ is a geodesic representative of the isotopy class of $(\mathcal{T}, \Gamma)$, concluding the proof of the first part of the theorem.

For the second statement, simply note that the convexity of the tiles to both sides of an edge forces the edge to be a geodesic. ◀

G Generating tilings

We briefly elaborate on the rational behind the construction of hyperbolic tilings. Since stellate groups are hyperbolic groups, they are shortlex biautomatic for any shortlex ordering for any finite generating set [6, 36]. Algorithms for automatic groups have been implemented in KBMAG [35] using GAP [30], and more recently, in MAF [73]. The algorithm attempts to produce a shortlex automatic structure for a group with a given presentation, using the set of generators given in the presentation [36, Section 5.4]. Using KBMAG and MAF, we implemented an algorithm that creates tilings of $\mathbb{H}^2$ using the data structure described in Section 4. We start with the construction of 1-fundamental tilings, for which we make use of the data structure described in Section 4, a single representative of each edge of the tiling is stored, relative to a set of generators, as a pair of vertices to be joined by a geodesic. These generators are expanded to a finite group presentation of the symmetry group, from which the algorithm creates a list $\mathcal{L}$ of words representing group elements, with each entry corresponding to a unique shortest word in the generators. The elements in $\mathcal{L}$ map the given edges to copies of themselves exactly once.

The goal of the creation of tilings is to create enough copies of the edges to cover the

given fundamental domain F_S for the surface S. This gives enough information to recover the embedding of the tile edges as a symmetric graph on S, by considering the overlay of the tiling with the edges of the edges of the fundamental domain. Our point of view in $\mathbb{H}^2$ is usually roughly centered around F_S as for the dodecagon in Figure 1, so the condition is approximately, up to some constant, equal to the condition that the applied transformations do not move points too far away from the focus. Now, the set of generators resulting from Step 3 in Algorithm 3 from which the construction starts is only defined up to conjugation in Γ [53, Theorem 2], so we can assume that every set results in some points of given edges to be in F_S. For stellate groups, we can even assume that each set of generators has a common generator with the starting set. The Cayley graph of a symmetry group w.r.t. to any (finite) set of generators $\mathcal{G}$ is quasi-isometric to $\mathbb{H}^2$ [27, Theorem 8.2], so there exists some constant $K_\mathcal{G}$ such that if an element $\gamma =_\Gamma a_1...a_n$ moves some vertex by a distance $\leq K_\mathcal{G}$, then any prefix of Γ displaces any generator by at most $k \leq K_\mathcal{G}$.

All in all, we see that by choosing the shortlex order, cutting off particular branches in $\mathcal{L}$ in a depth-first search after some given threshold will not result in the tiling missing copies within a certain radius around the starting edges. The cut-off point is determined experimentally for each set of generators. Finally, the edges are produced by filling in the geodesics between vertices. Note that, in the Poincaré model, choosing the points interpolating the edges to be equally spaced w.r.t. the Euclidean distance yields a more robust implementation of the procedure than using the hyperbolic distance, as distances towards the edge of the unit circle become more and more distorted. The rest of the produced tiling outside of F_S can be trimmed by considering which points lie outside the circles defining the boundary of F_S. Example of graphs in the dodecagon resulting from tilings are illustrated in Figure 16.

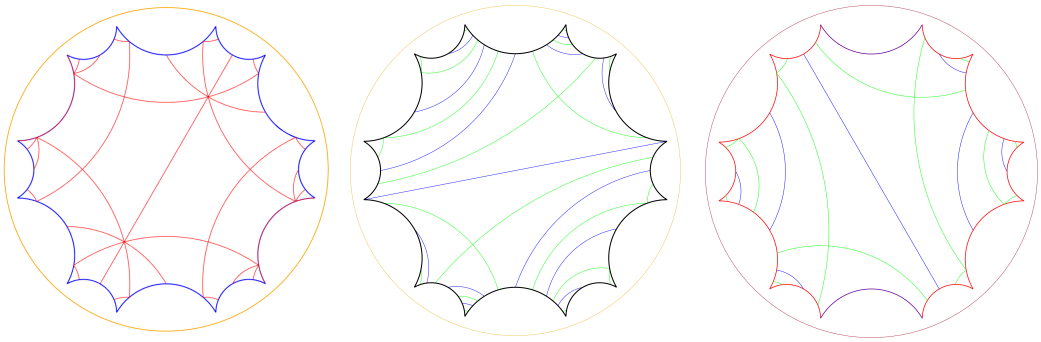

Figure 16 Tilings with symmetry group 2224 in the dodecagon. Left: The tiling in Figure 10(left).